Atmos. Chem. Phys., 17, 7807–7826, 2017
https://doi.org/10.5194/acp-17-7807-2017

Atmospheric Chemistry and Physics
Open Access
EGU

Estimating the atmospheric concentration of Criegee intermediates and their possible interference in a FAGE-LIF instrument

Anna Novelli[1,a], Korbinian Hens[1], Cheryl Tatum Ernest[1,b], Monica Martinez[1], Anke C. Nölscher[1,c], Vinayak Sinha[2], Pauli Paasonen[3], Tuukka Petäjä[3], Mikko Sipilä[3], Thomas Elste[4], Christian Plass-Dülmer[4], Gavin J. Phillips[1,5], Dagmar Kubistin[1,4,6], Jonathan Williams[1], Luc Vereecken[1,a], Jos Lelieveld[1], and Hartwig Harder[1]

[1]Atmospheric Chemistry Department, Max Planck Institute for Chemistry, 55128 Mainz, Germany
[2]Department of Earth and Environmental Sciences, Indian Institute of Science Education and Research Mohali, Sector 81 S.A.S. Nagar, Manauli PO, Mohali 140 306, Punjab, India
[3]Department of Physics., P.O. Box 64. 00014 University of Helsinki, Helsinki, Finland
[4]German Meteorological Service, Meteorological Observatory Hohenpeissenberg (MOHp), 83282 Hohenpeissenberg, Germany
[5]Department of Natural Sciences, University of Chester, Thornton Science Park, Chester, CH2 4NU, UK
[6]University of Wollongong, School of Chemistry, Wollongong, Australia
[a]now at: Institute of Energy and Climate Research, IEK-8: Troposphere, Forschungszentrum Jülich GmbH, 52428 Jülich, Germany
[b]now at: Department of Neurology University Medical Center of the Johannes Gutenberg University Mainz, 55131 Mainz, Germany
[c]now at: Division of Geological and Planetary Sciences, California Institute of Technology, Pasadena, USA

Correspondence to: Hartwig Harder (hartwig.harder@mpic.de)

Received: 11 October 2016 – Discussion started: 24 October 2016
Revised: 2 May 2017 – Accepted: 19 May 2017 – Published: 29 June 2017

Abstract. We analysed the extensive dataset from the HUMPPA-COPEC 2010 and the HOPE 2012 field campaigns in the boreal forest and rural environments of Finland and Germany, respectively, and estimated the abundance of stabilised Criegee intermediates (SCIs) in the lower troposphere. Based on laboratory tests, we propose that the background OH signal observed in our IPI-LIF-FAGE instrument during the aforementioned campaigns is caused at least partially by SCIs. This hypothesis is based on observed correlations with temperature and with concentrations of unsaturated volatile organic compounds and ozone. Just like SCIs, the background OH concentration can be removed through the addition of sulfur dioxide. SCIs also add to the previously underestimated production rate of sulfuric acid. An average estimate of the SCI concentration of $\sim 5.0 \times 10^4$ molecules cm^{-3} (with an order of magnitude uncertainty) is calculated for the two environments. This implies a very low ambient concentration of SCIs, though, over the boreal forest, significant for the conversion of SO_2 into H_2SO_4. The large uncertainties in these calculations, owing to the many unknowns in the chemistry of Criegee intermediates, emphasise the need to better understand these processes and their potential effect on the self-cleaning capacity of the atmosphere.

1 Introduction

Criegee intermediates (CIs), or carbonyl oxides, are formed during the ozonolysis of unsaturated organic compounds (Criegee, 1975; Johnson and Marston, 2008; Donahue et al., 2011): in the gas phase, ozone attaches to a double bond, forming a primary ozonide (POZ) that quickly decomposes forming a Criegee intermediate and a carbonyl compound. The CIs can exist as thermally stabilised CIs (SCIs) or as chemically activated CIs (Kroll et al., 2001; Drozd et al., 2011), where the chemically activated CIs have high energy content and in the atmosphere either undergo unimolecular

decomposition or are stabilised by collisional energy loss forming SCIs.

For many decades the chemistry of Criegee intermediates was investigated with both theoretical and indirect experimental studies as reviewed in detail by Johnson and Marston (2008), Vereecken and Francisco (2012), and Vereecken et al. (2015). During the last few years, numerous experimental studies specifically on stabilised Criegee intermediates have been performed following their first detection by Welz et al. (2012). Many laboratories have now detected SCIs with various techniques (Berndt et al., 2012; Mauldin III et al., 2012; Ouyang et al., 2013; Taatjes et al., 2013; Ahrens et al., 2014; Buras et al., 2014; Liu et al., 2014a; Sheps et al., 2014; Novelli et al., 2014b; Stone et al., 2014; Chhantyal-Pun et al., 2015; Lee, 2015; Newland et al., 2015a; Fang et al., 2016a; Smith et al., 2016) and have confirmed that they are very reactive towards many atmospheric trace gases. Currently, the most studied Criegee intermediates are formaldehyde oxide, CH_2OO; acetaldehyde oxide, CH_3CHOO (*syn* and *anti*, i.e. with the outer oxygen pointing towards or away from an alkyl group, respectively); and acetone oxide, $(CH_3)_2COO$.

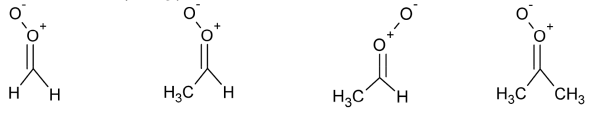

The importance of stabilised Criegee intermediates as oxidants in the atmosphere depends on the rate coefficient of their reaction with water vapour as the latter is ubiquitously present in relatively high concentrations in the boundary layer (between 10^{16} and 10^{17} molecules cm^{-3}). The rate of this reaction strongly depends on the CI conformation (Aplincourt and Ruiz-López, 2000; Tobias and Ziemann, 2001; Ryzhkov and Ariya, 2003; Kuwata et al., 2010; Anglada et al., 2011; Anglada and Sole, 2016; Chen et al., 2016; Lin et al., 2016; Long et al., 2016) and until now the rate coefficient has been measured for *anti*-CH_3CHOO (Taatjes et al., 2013; Sheps et al., 2014), while lower limits have been determined for CH_2OO (Stone et al., 2014), *syn*-CH_3CHOO (Taatjes et al., 2013; Sheps et al., 2014), and $(CH_3)_2COO$ (Huang et al., 2015; Newland et al., 2015b). The uncertainties in these rate coefficients make it difficult to estimate the importance of Criegee intermediates and the impact they may have as oxidants in the atmosphere. Additionally, recent studies (Berndt et al., 2014b; Chao et al., 2015; Lewis et al., 2015; Smith et al., 2015; Lin et al., 2016) have showed that the reaction between CH_2OO and water dimers (present in the ppmv range in the atmosphere; Shillings et al., 2011) is faster than the reaction with water vapour, in agreement with the several theoretical studies (Ryzhkov and Ariya, 2004; Chen et al., 2016; Lin et al., 2016) which indicate the reaction with water dimers to be between 400 and 35 000 times faster than the reaction with water vapour depending on the conformers. Another important reaction of SCIs that depends on the SCI conformation is their unimolecular decomposition. The decomposition rate and product formed depend on the SCI conformer structure. *anti*-SCIs are likely to isomerise via the ester channel forming an ester or an acid as the final product, while *syn*-SCIs will form a vinyl hydroperoxide (VHP) which promptly decomposes forming hydroxyl radicals (OH) and a vinoxy radical (Paulson et al., 1999; Johnson and Marston, 2008; Drozd and Donahue, 2011; Vereecken and Francisco, 2012; Kidwell et al., 2016). Larger and more complex conformers such as heterosubstituted or cyclic structures are subject to additional unimolecular rearrangements (Vereecken and Francisco, 2012). On the unimolecular decomposition rates and products few experimental data are available (Horie et al., 1997, 1999; Fenske et al., 2000a; Novelli et al., 2014b; Kidwell et al., 2016; Fang et al., 2016a; Smith et al., 2016), but more is available from theoretical studies explicitly focusing on the path followed by different conformers (Anglada et al., 1996; Aplincourt and Ruiz-López, 2000; Kroll et al., 2001; Zhang and Zhang, 2002; Nguyen et al., 2009b; Kuwata et al., 2010).

Most of the experimental and theoretical information described above refers to the smaller conformers. These compounds are likely to be formed relatively efficiently in the atmosphere as they can originate from any unsaturated compound with a terminal double bond, but they do not represent the entire Criegee intermediate population.

As SCIs were found to react quickly with many trace gases, various model studies were performed on the impact SCIs have as oxidants in the atmosphere (Vereecken et al., 2012; Boy et al., 2013; Percival et al., 2013; Pierce et al., 2013; Sarwar et al., 2013, 2014; Novelli et al., 2014b; Vereecken et al., 2014). Some of these studies focused in particular on the possible impact that SCIs might have on the formation of sulfuric acid (H_2SO_4) in the gas phase, following Mauldin III et al. (2012), who suggested that Criegee intermediates are the missing SO_2 oxidant needed to close the sulfuric acid budget over a boreal forest. This is supported by theoretical and laboratory studies that have determined a rate coefficient between SCIs and sulfur dioxide (SO_2) of the order of 10^{-11} cm^3 molecule^{-1} s^{-1} (Aplincourt and Ruiz-López, 2000; Jiang et al., 2010; Kurteìn et al., 2011; Vereecken et al., 2012; Welz et al., 2012; Taatjes et al., 2013; Liu et al., 2014b; Sheps et al., 2014; Stone et al., 2014). As the main atmospherically relevant oxidiser of SO_2 in the gas phase is the OH radical with a rather slow rate coefficient at ambient temperature and pressure of 2×10^{-12} cm^3 molecule^{-1} s^{-1} (Atkinson et al., 2004), the high rate coefficient for SO_2 oxidation would allow SCIs to have a significant impact on the H_2SO_4 formation even if present in small concentrations. The model studies have shown that, depending on the environment, SCIs can have a potentially important impact on H_2SO_4 formation. All these studies are affected by large uncertainties and many simplifications used for coping with the paucity of data on the reac-

tions of specific SCIs with various trace gas species, on the speciation of SCIs, and on the steady-state concentration of SCIs in the troposphere. Until now no direct or reproducible indirect method has been able to determine the steady-state concentration of SCIs in the lower troposphere.

In this paper, we firstly estimate the concentration of SCIs in the lower troposphere, based on the data collected during the HUMPPA-COPEC 2010 campaign (Williams et al., 2011) in a boreal forest in Finland and the HOPE 2012 campaign in rural southern Germany. The budget of SCIs is analysed using four different approaches: (1) based on an unexplained H_2SO_4 production rate (Mauldin III et al., 2012); (2) from the measured concentrations of unsaturated volatile organic compounds (VOCs); (3) from the observed OH reactivity (Nölscher et al., 2012); and (4) from an unexplained production rate of OH (Hens et al., 2014). Secondly, we present measurements obtained using our inlet pre-injector laser-induced fluorescence assay by gas expansion technique (IPI-LIF-FAGE) (Novelli et al., 2014a) during the HUMPPA-COPEC 2010 and the HOPE 2012 campaigns. A recent laboratory study performed with the same instrumental setup showed that the IPI-LIF-FAGE system is sensitive to the detection of the OH formed from unimolecular decomposition of SCIs (Novelli et al., 2014b). Building on this study, the background OH (OH_{bg}) (Novelli et al., 2014a) measured during the two field campaigns is investigated in comparison with many other trace gases in order to assess whether the observations in controlled conditions are transferable to the ambient conditions.

2 Instrumentation and field sites

2.1 IPI-LIF-FAGE description

A comprehensive description of the IPI-LIF-FAGE ground-based instrument, HORUS (Hydroxyl Radical Measurement Unit based on fluorescence Spectroscopy), is given by Novelli et al. (2014a) and only some important features of the instrument are highlighted here. The IPI-LIF-FAGE instrument consists of the inlet pre-injector (IPI), the inlet and detection system, the laser system, the vacuum system, and the instrument control and data acquisition unit. The air is drawn through a critical orifice into a low-pressure region ($\sim$ 300–500 Pa) where OH molecules are selectively excited by pulsed UV light around 308 nm. The light is generated at a pulse repetition frequency of 3 kHz by a Nd:YAG pumped, pulsed, tunable dye laser system and is directed into a multipass "White cell" making 32 passes through the detection volume (White, 1942). The air sample intersects the laser beam and the fluorescence signal from the excited OH molecules is detected using a gated micro-channel plate (MCP) detector. The IPI, situated in front of the instrument inlet, is used to measure a chemical zero to correct for possible internal OH signal generation. An OH scavenger (propene) is added to the sample air 5 cm in front of the inlet pinhole in a concentration that allows a known, high proportion of atmospheric OH to be scavenged ($\sim$ 90 %). The OH scavenger is added every 2 min so that the instrument measures a total OH signal (OH_{tot}) when the OH scavenger is not injected and a background OH signal (OH_{bg}) when the OH scavenger is injected. The difference between these two signals yields the atmospheric OH concentration (OH_{atm}). The efficiency of this technique for measuring OH with this particular LIF-FAGE instrument is described together with the IPI characterisation in Novelli et al. (2014a). The OH calibration of the HORUS instrument is obtained via the production of a known amount of OH and hydroperoxyl radicals (HO_2) from the photolysis of water at 185 nm using a mercury lamp. A more detailed description of the instrument calibration is reported by Martinez et al. (2010) and Hens et al. (2014). A calibration factor for the background OH signal observed by the HORUS instrument is currently not available. Therefore, this signal will be discussed and plotted in OH fluorescence counts per second measured by the MCP, normalised by the laser power and corrected for quenching and sensitivity changes towards the detection of OH. The sensitivity of the instrument towards the OH radical is affected by alignment of the white cell, optical transmission of the components, sensitivity of the MCP, water vapour, internal pressure, and internal temperature (Martinez et al., 2010). These factors affect the sensitivity of HORUS towards the background OH in a similar manner as they mainly impact the sensitivity of the instrument to the detection of OH.

We hypothesise that the OH_{bg} is formed chemically within the IPI-LIF-FAGE instrument. Laser-induced production of OH radicals was thoroughly tested in the laboratory and in the field (Novelli et al., 2014a), showing that this background OH signal is not induced by the laser beam from double pulsing, nor from air stagnating in the detection cell. By changing the laser power, no quadratic dependency of the OH_{bg} was observed even at night time, when the contribution of the OH_{bg} to the OH_{tot} measured by the instrument is highest (Novelli et al., 2014a). In addition, during the HUMPPA-COPEC 2010 and HOPE 2012 campaigns, the correlation coefficient of the OH_{bg} with the laser power was $R = 0.002$ and $R = 0.2$, respectively.

In contrast, ozonolysis of alkenes performed during laboratory tests showed that the IPI-LIF-FAGE instrument is sensitive to the OH formed from unimolecular decomposition of SCIs within the low-pressure section of the instrument (Novelli et al., 2014b).

Recently, most of the LIF-FAGE instruments have been augmented with the titration of OH_{atm} in different environments to determine their background (Amédro, 2012; Mao et al., 2012; Griffith et al., 2013, 2016; Woodward-Massey et al., 2015; Tan et al., 2017). Some of these instruments showed the presence of an unknown interference (Mao et al., 2012; Griffith et al., 2013; Tan et al., 2017), while for others no clear conclusions were drawn (Amédro, 2012;

Woodward-Massey et al., 2015). In addition, laboratory studies (Fuchs et al., 2016; Griffith et al., 2016) have shown similarity with what was observed with the IPI-LIF-FAGE during experiments of ozonolysis of alkenes, although the origin of the OH signal was not uniquely attributed to a particular mechanism.

Our hypothesis is that the OH_{bg} measured in ambient air with the IPI-LIF-FAGE at least partially originates from unimolecular decomposition of SCIs. Section 4 describes the observed behaviour of the signal during the campaigns and its relationship to other observed chemical tracers and discusses whether this is compatible with our hypothesis.

2.2 Measurement site and ancillary instrumentation

We present measurements from two sites, a boreal forest site in Finland and a rural site in southern Germany. The HUMPPA-COPEC 2010 (Hyytiälä United Measurements of Photochemistry and Particles in Air – Comprehensive Organic Precursor Emission and Concentration study) campaign took place during summer 2010 at the SMEAR II station in Hyytiälä, Finland (61°51′ N, 24°17′ E; 181 m a.s.l.) in a boreal forest dominated by Scots pines (*Pinus silvestris* L.). The site hosts continuous measurements of several trace gases and meteorological parameters as well as aerosol particles concentrations, size distributions, and composition (Junninen et al., 2009). Further details and a more complete description of the site, the instrumentation, and the meteorological conditions during the campaign can be found in Williams et al. (2011) and Hens et al. (2014). A brief description of the instruments used in this study is given here. Ozone was measured by a UV photometric gas analyser (model 49, Thermo Electron Corporation). A gas chromatograph (GC, Agilent Technologies 6890A) coupled to a mass-selective detector (MS, Agilent Technologies MSD 5973 *inert*) was used for the measurements of biogenic volatile organic compounds (BVOCs) (Yassaa et al., 2012). The total OH reactivity was measured by the comparative reactivity method (CRM) (Sinha et al., 2008) for two different heights, one within and one above the canopy (18 and 24 m, respectively) (Nölscher et al., 2012). CRM uses an in situ kinetics experiment to measure the OH reactivity based on the competitive scavenging of OH by a reference gas (pyrrole) and atmospheric OH reactants. The overall uncertainty of the method during deployment was 16 %, with a limit of detection of $3.0\,s^{-1}$ (Hens et al., 2014). Sulfur dioxide (SO_2) concentration was measured with a fluorescence analyser (model 43S, Thermo 20 Environmental Instruments Inc.). Aerosol number size distributions between 3.0 and 950 nm were measured with a differential mobility particle sizer (DMPS) (Aalto et al., 2001). The size distributions were used for calculating the loss rate of gas-phase sulfuric acid via condensation sink (CS) with the method presented by Kulmala et al. (2001). Sulfuric acid (H_2SO_4) and OH radical concentrations were measured on the ground with a chemical ionisation mass spectrometer (CIMS; Petäjä et al., 2009). Time series of the measured trace gases are available in the study from Nölscher et al. (2012) and Hens et al. (2014). The average concentrations and their 1σ variability are listed in Tables 1 and S2 in the Supplement. For the first period of the campaign, between 27 and 31 July, the IPI-LIF-FAGE instrument was run on the ground side by side with the CIMS. On 2 August the IPI-LIF-FAGE instrument was moved to the top of the HUMPPA tower above the canopy and measured there for the remainder of the campaign (12 August). The data are therefore separated into ground and tower periods

Table 1. Average concentration (molecules cm^{-3}), with 1σ variability, of trace gases relevant for this study.

Compound	HUMPPA-COPEC 2010	HOPE 2012
SO_2[a]	$(1.4 \pm 1.7) \times 10^{10}$	$(2.2 \pm 2.3) \times 10^{9}$
H_2SO_4[a]	$(2.0 \pm 2.0) \times 10^{6}$	$(8.5 \pm 8.5) \times 10^{5}$
OH[a]	$(7.0 \pm 8.0) \times 10^{5}$	$(1.6 \pm 1.6) \times 10^{6}$
O_3[a]	$(1.1 \pm 0.2) \times 10^{12}$	$(1.1 \pm 0.3) \times 10^{12}$
Σ[VOC][a,b]	$(7.3 \pm 7.1) \times 10^{9}$	$(9.8 \pm 9.0) \times 10^{9}$
OH reactivity[c]	9.0 ± 7.6	3.5 ± 3.0
Condensation sink (CS)[c]	$(10 \pm 4.0) \times 10^{-3}$	$(7.0 \pm 3.0) \times 10^{-3}$

[a] Units: molecules cm^{-3}. [b] HUMPPA COPEC 2010: isoprene, ±α-pinene, ±β-pinene, 3-carene, and myrcene. HOPE 2012: isoprene, α-pinene, β-pinene, 3-carene, myrcene, limonene, 2-methylpropene, but-1-ene, sabinene, γ-terpinene, propene, *cis*-2-butene and ethene. [c] Units: s^{-1}. 1 ppbv = 2.5×10^{10} molecules cm^{-3} at 295 K and 1013 hPa.

The HOPE 2012 (Hohenpeißenberg Photochemistry Experiment) campaign was conducted during the summer of 2012 at the Meteorological Observatory in Hohenpeissenberg, Bavaria, Germany (47°48′ N, 11°2′ E). The observatory is a Global Atmosphere Watch (GAW) station operated by the German Meteorological Service (DWD) and is located at an altitude of 985 m a.s.l. and about 300 m above the surrounding terrain, mainly consisting of meadows and coniferous forests. More information about the site can be found in Handisides et al. (2003). Ozone was measured by UV absorption with a TEI 49C (Thermo Electron Corporation, Environmental Instruments) (Gilge et al., 2010). Nonmethane hydrocarbons were measured with a GC–flame ionisation detection (FID) system (series 3600CX, Varian, Walnut Creek, CA, USA) (Plass-Dülmer et al., 2002). BVOCs were detected using a GC (Agilent 6890) with a FID running in parallel with a MS (Agilent Technologies MSD 5975 *inertXL*) described by Hoerger et al. (2015). Photolysis frequencies ($J(NO_2)$ and $J(O^1D)$) were measured next to the IPI-LIF-FAGE with a set of filter radiometers (Handisides et al., 2003). The OH reactivity was measured with two instruments for a short period of time from 10 until 18 July. One method was the CRM and the same instrument was used as during the HUMPPA-COPEC 2010 campaign. The second method was a new application of the DWD CIMS instrument (Berresheim et al., 2000) which also measured H_2SO_4 and OH radicals. As the data will be used only in a qualitative way for the current study, a very short description of this novel technique is given here and details will be presented in

Table 2. SCI estimates for the HUMPPA-COPEC 2010 and HOPE 2012 campaigns. Average concentration (molecules cm^{-3}), with 1σ variability.

Approach	HUMPPA-COPEC 2010	HOPE 2012
Missing H_2SO_4	$(2.3 \pm 2.0) \times 10^4$ [a]	$(2.0 \pm 3.0) \times 10^4$ [a]
	$(1.6 \pm 2.0) \times 10^6$ [b]	$(1.0 \pm 3.0) \times 10^6$ [b]
Measured unsaturated VOCs	$(5.0 \pm 4.0) \times 10^3$	$(7.0 \pm 6.0) \times 10^3$
Unexplained OH reactivity	$(1.0 \pm 1.0) \times 10^5$	$(2.0 \pm 1.5) \times 10^4$
Unexplained OH production	$(2.0 \pm 2.0) \times 10^4$ [c]	n/a
	$(4.0 \pm 4.0) \times 10^5$ [d]	n/a

[a] $k_{SCI+SO_2} = 3.3 \times 10^{-11}$ cm^3 $molecule^{-1}$ s^{-1} [b] $k_{SCI+SO_2} = 5.0 \times 10^{-13}$ cm^3 $molecule^{-1}$ s^{-1}
[c] $P_{OH}^{unexplained} = 1.0 \times 10^6$ molecules cm^{-3} s^1 [d] $P_{OH}^{unexplained} = 2.0 \times 10^7$ molecules cm^{-3} s^1
1 ppbv $= 2.5 \times 10^{10}$ molecules cm^{-3} at 295 K and 1013 hPa. n/a: not applicable.

a future publication. With the CIMS instrument, OH radicals are measured by converting them into H_2SO_4 after reaction with SO_2 in a chemical reactor and subtraction of a corresponding background after scavenging the OH with propane (Berresheim et al., 2000). A second SO_2 titration zone was used 15 cm (or 140 ms) downstream of the first injection to determine the OH decay from OH radicals generated in the UV-calibration zone immediately upstream of the first titration. The difference between these two titration zones in two consecutive 2.5 min intervals allows the determination of the OH decay, after correcting for ambient OH and wall losses. The uncertainty is estimated at $\pm 2.0\,s^{-1}$ and the limit of detection is $2.0\,s^{-1}$. SO_2 concentration was measured with a fluorescence analyser and aerosol size distributions were measured and used to calculate the loss rate of gas-phase sulfuric acid due to CS formed by existing aerosol surface via the method presented by Birmili et al. (2003). Time series of the measured trace gases are available in Fig. S1 in the Supplement. The average concentrations and their 1σ variability are listed in Tables 1 and 2.

3 SCI concentrations during HUMPPA-COPEC 2010 and HOPE 2012

3.1 Missing H_2SO_4 oxidant

The study by Mauldin III et al. (2012) in a boreal forest during the HUMPPA-COPEC 2010 campaign showed a consistent discrepancy between the measured H_2SO_4 and the calculated gas-phase H_2SO_4 concentration when considering oxidation of SO_2 from OH radical and the condensation onto pre-existing aerosol particles (CS, condensation sink) as the sole production and loss processes, respectively (Eq. 1).

$$[H_2SO_4] = \frac{k_{OH+SO_2} \times [OH] \times [SO_2]}{CS} \quad (1)$$

The H_2SO_4 concentration is assumed to be in near-steady state: the lifetime of H_2SO_4 in the gas phase is of the order of minutes, i.e. spanning a similar time period compared to the variability in the production and loss pathways, ensuring fast response of the H_2SO_4 concentration to varying conditions. Minor deviations from steady state are not critical for the analysis performed in this study, given the uncertainties induced by other parameters.

On average the sulfuric acid in the gas phase calculated using Eq. (1) was only half of the total H_2SO_4 observed in the field and lay outside the uncertainties associated with the calculation of the formation channel and the condensation sink (Mauldin III et al., 2012). Although no unambiguous evidence links SCIs to the missing oxidant, laboratory tests performed with a similar instrument (Berndt et al., 2012, 2014a; Sipilä et al., 2014) confirmed the role that SCIs could have in the oxidation of SO_2 and formation of H_2SO_4. Assuming that SCIs are the only other species in addition to OH that oxidise SO_2 in the gas phase and knowing the rate coefficient of SCIs and OH with SO_2, it is possible to calculate the steady-state concentration of SCIs in that environment:

$$[H_2SO_4] = \frac{(k_{OH+SO_2} \times [OH] + k_{SCI+SO_2} \times [SCI]) \times [SO_2]}{CS}. \quad (2)$$

The rate coefficient between OH and SO_2 at standard pressure is $(2.0 \pm 0.1) \times 10^{-12}$ $(T/300)^{-0.27}$ cm^3 $molecule^{-1}$ s^{-1} (Atkinson et al., 2004). The rate coefficient of SCIs with SO_2 was determined by several groups at $(3.3 \pm 2.0) \times 10^{-11}$ cm^3 $molecule^{-1}$ s^{-1} (Welz et al., 2012; Taatjes et al., 2013; Liu et al., 2014b; Sheps et al., 2014; Stone et al., 2014; Chhantyal-Pun et al., 2015; Newland et al., 2015a, b; Foreman et al., 2016; Zhu et al., 2016). An earlier, lower value of $\sim 5.0 \times 10^{-13}$ cm^3 $molecule^{-1}$ s^{-1} (Mauldin III et al., 2012; Berndt et al., 2012) appears to be hard to reconcile with the remaining literature, as extensively discussed in the Supplement.

Equation (2) allows for the calculation of a time series of SCIs (Fig. S2), yielding an average $[SCI] = (2.3 \pm 2.0) \times 10^4$ molecules cm^{-3}. A similar estimate of the SCI time series was derived for the HOPE 2012 campaign (Fig. S3). These time series are discussed in more detail in the Supplement; for the estimation of atmospheric SCIs here we focus mostly on the overall concentration.

The H_2SO_4 concentration during this campaign can be mainly explained by the reaction between OH and SO_2. Figure 1 shows the correlation between the total production rate of H_2SO_4 ($P(H_2SO_4)_{tot}$) calculated from the product of measured H_2SO_4 and the condensation sink, as well as the production rate of H_2SO_4 from the reaction of OH and SO_2. The linear regression following the method of York et al. (2004) yields a slope of 0.9 ± 0.02 with a negligible intercept (57 ± 7.0 molecules cm^{-3} s^{-1}). It should be noted that the H_2SO_4 budget for the HOPE 2012 campaign is nearly closed, such that the moderate fluctuations on the source data (CS, [OH], etc.) lead to very large relative uncertainties of the small missing H_2SO_4 production term,

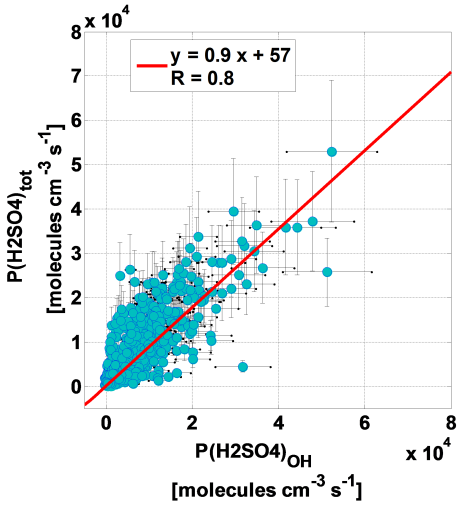

Figure 1. Total production rate of H_2SO_4 ($P(H_2SO_4)_{tot}$) as a function of the production rate of H_2SO_4 from the reaction between OH and SO_2 during the HOPE 2012 campaign. The linear regression, following the method of York et al. (2004), yields a slope of 0.9 ± 0.02 and a intercept of 57 ± 7.

and concomitantly the time series for the SCI concentration (Fig. S3) shows extreme variability reflecting this noise on the source data. On average, the [SCI] obtained is low, $(2.0 \pm 3.0) \times 10^4$ molecules cm^{-3}, with no values in the time series exceeding 10^5 molecules cm^{-3}.

Repeating the above analysis using the low k_{SCI+SO_2} value of Mauldin III et al. (2012) and Berndt et al. (2014) yields concentrations of $(1.6 \pm 2.0) \times 10^6$ and $(1.0 \pm 3.0) \times 10^6$ molecules cm^{-3} for the HUMPPA-COPEC and HOPE campaigns, respectively. It is interesting to note that both values estimated with the fast and low k_{SCI+SO_2} rate coefficient are in agreement with the concentrations calculated from measured VOCs and O_3 for polluted and pristine environments, 1.9×10^6 and 4.5×10^4 molecules cm^{-3} respectively, from a previous study (Welz et al., 2012).

3.2 Measured unsaturated VOCs

Another method to estimate the SCI concentration is based on their production and loss processes. In a forest SCIs are expected to be formed from the ozonolysis of unsaturated BVOCs. It is possible to calculate an average steady-state concentration for SCIs using the following equation

$$[\mathrm{SCI}] = \sum_i \left(\frac{k_{\mathrm{VOC}_i+\mathrm{O_3}} \times [\mathrm{VOC}_i] \times Y_{\mathrm{SCI}}}{L_{\mathrm{SCI_{syn}}}} \right) \times [\mathrm{O_3}], \qquad (3)$$

where $k_{\mathrm{VOC}_i+\mathrm{O_3}}$ is the rate coefficient between the VOC_i and ozone (Table S2), Y_{SCI} is the yield of SCIs in the ozonolysis reaction, and L_{SCIsyn} is the total loss of *syn*-SCI. We assume $[SCI] \approx [SCI_{syn}]$ following the model described by Novelli et al. (2014b), which accounts for many possible losses of SCIs, including the reaction with water dimers and unimolecular decomposition. The latter study suggests that *anti*-acetaldehyde oxide and formaldehyde oxide react quickly with water and water dimers and that their contributions can be neglected. A yield of SCI formation (Y_{SCI}) of 0.4 was estimated based on the data by Hasson et al. (2001). The steady-state concentration of SCIs for the HUMPPA-COPEC 2010 campaign was calculated using the measured data for $[O_3]$ and $[VOC_i]$, and an average value of 40 s^{-1} (Novelli et al., 2014b) for L_{SCIsyn} as this value was found to be rather constant and mainly dependent on the unimolecular decomposition rate of the SCIs. Equation (3) allows for the calculation of a time series of SCIs (Fig. S4) yielding an average [SCI] of $\sim (5.0 \pm 4.0) \times 10^3$ molecules cm^{-3}. These time series are discussed in more detail in the supporting information; for the estimation of atmospheric SCIs here we focus mostly on the overall concentration.

During the HOPE 2012 campaign a larger number of unsaturated organic trace gases, both anthropogenic and biogenic, were measured (Table S1). For Y_{SCI} the same value of 0.4 was used, while for L_{SCIsyn} the value of 32 s^{-1}, obtained from the model described by Novelli et al. (2014b) for the rural European environment, was used. Using these values in Eq. (3) results in $[SCI] = (7.0 \pm 6.0) \times 10^3$ molecules cm^{-3}, obtained as an average of the SCI time series (Fig. S5). It should be noted that recent work on the unimolecular decomposition (Fang et al., 2016b; Long et al., 2016; Smith et al., 2016) yields loss rates significantly faster than used here; this implies that the [SCI] obtained here could be an overestimate.

3.3 OH reactivity

During HUMPPA-COPEC 2010, between 27 July and 12 August, an average OH reactivity of $R = 9.0 \pm 7.6$ s^{-1} was measured. On average, the majority of the measured OH reactivity ($R_{unex} = 7.4 \pm 7.4$ s^{-1}, i.e. 80 %) was not accounted for by the measured organic and inorganic trace gases (Fig. S6). Biogenic emissions comprised up to ~ 10 % of the total measured OH reactivity and up to half of the calculated OH reactivity (Fig. S6). As the measurement site was located in a pristine forest environment, affected only little by anthropogenic emissions (Williams et al., 2011), it is likely that a large fraction of the unexplained OH reactivity was formed by unmeasured primary emissions by the vegetation and secondary products of oxidation. By assuming that the unmeasured VOCs are unsaturated, and by using a lumped rate coefficient, k_{VOC+OH}, between OH and the fraction of unspeciated VOCs of 7.0×10^{-11} cm^3 molecule^{-1} s^{-1}, typical for an OH addition to a carbon–carbon double bond (Atkinson et al., 2004; Peeters et al., 2007), it is possible to estimate the concentration $[VOC_{unknown}]$ of VOCs that

would be necessary to close the OH reactivity budget (Eq. 4).

$$R_{\mathrm{unex}} = k_{\mathrm{VOC+OH}} \times [\mathrm{VOC_{unknown}}] \quad (4)$$

Using Eq. (4), a time series for $[\mathrm{VOC_{unknown}}]$ with an average of $(1.0 \pm 1.0) \times 10^{11}$ molecules cm^{-3} is obtained. These values are substituted into Eq. (3) and a lumped rate coefficient k of 7.0×10^{-17} molecules cm^{-3} is used for reaction of $[\mathrm{VOC_{unknown}}]_t$ with $[\mathrm{O_3}]_t$ at time t. This k value is based on the rate coefficient of the measured VOCs with O_3 weighted with their abundance (Table S1). The same Y_{SCI} and L_{SCIsyn}, of 0.4 and 40 s^{-1}, respectively, were used as described in Sect. 3.2. With these values, a time series of SCIs (Fig. S7) with an average of $\sim(1.0 \pm 1.0) \times 10^5$ molecules cm^{-3} is obtained. To this SCI concentration estimate, we add the SCIs formed from the measured unsaturated VOCs, $[\mathrm{SCI}] = (5.0 \pm 4.0) \times 10^3$ molecules cm^{-3}, to obtain the total SCIs across all VOCs. As this estimate requires assumptions for the rate coefficient between $[\mathrm{VOC_{unknown}}]$ and OH and O_3, a sensitivity study probing the upper and lower bounds of this estimate is described in the Supplement. The time series are discussed in more detail in the Supplement; for the estimation of atmospheric SCIs here we focus mostly on the overall concentration.

During the HOPE 2012 campaign the total OH reactivity was on average 3.5 ± 3.0 s^{-1}. Using the measured trace gas concentrations it is possible to calculate the expected OH reactivity (Fig. S8). Table S2 lists all the species included in the calculation of the OH reactivity with their rate coefficient with OH. An average value of 2.7 ± 0.7 s^{-1} was calculated. Figure S8 shows that half of the measured OH reactivity can be explained by methane, carbonyl compounds (mainly acetaldehyde and propanal), and inorganic compounds which were present in higher concentrations compared to the HUMPPA-COPEC 2010 campaign (Table S2). On average, 24 % of the measured OH reactivity remains unexplained by the measured trace gases. In contrast to the HUMPPA-COPEC 2010 campaign, in HOPE 2012 a more complete speciation of VOCs was measured (Table S1) and the site was influenced by relatively fresh anthropogenic emissions. With the extensive VOC speciation available, the reactivity budget can virtually be closed, but any remaining unexplained OH reactivity could still be due to unmeasured VOCs. The time series for this unexplained OH reactivity, typically about ~ 1 s^{-1}, shows very large variability as it reflects the statistical noise of the small difference between measured and calculated OH reactivities, both of which are associated with variability. The resulting [SCI] time series (Fig. S9) is also highly variable, and yields a low average SCI concentration of $(2.0 \pm 1.5) \times 10^4$ molecules cm^{-3}, with no values exceeding 6.0×10^4 molecules cm^{-3}.

The total of SCIs is then obtained by summing the SCIs predicted from the measured VOCs and from the unexplained OH reactivity, leading to a total SCI concentration of $(7.0 \pm 6.0) \times 10^3$ molecules cm^{-3}.

3.4 Unexplained OH production rate

During the HUMPPA-COPEC 2010 campaign, the comprehensive measurements (Williams et al., 2011) allowed the calculation of a detailed OH budget (Hens et al., 2014). Most of the OH production during daytime is due to photolysis of O_3 and recycling of HO_2 back to OH via reactions with NO and O_3. This result holds for both high ($R > 15$ s^{-1}) and low ($R \leq 15$ s^{-1}) OH reactivity episodes during the campaign. While the OH budget can be closed during daytime ($\mathrm{J(O^1D)} > 3.0 \times 10^{-6}$ s^{-1}) for low OH reactivity periods, during periods with high OH reactivity there was a large unexplained production rate of OH, $P_{\mathrm{OH}}^{\mathrm{unexplained}} = (2.0 \pm 0.7) \times 10^7$ molecules cm^{-3} s^{-1}, which can thus be surmised to originate from VOC chemistry. In addition, for both periods, during night time ($\mathrm{J(O^1D)} \leq 3.0 \times 10^{-6}$ s^{-1}), the IPI-LIF-FAGE and the CIMS instruments both measured non-negligible OH concentrations (Hens et al., 2014) where most of the OH production was from unknown sources ($P_{\mathrm{OH}}^{\mathrm{unexplained}} = 1.0 \pm 0.9 \times 10^6$ molecules cm^{-3} s^{-1} (1σ) and $P_{\mathrm{OH}}^{\mathrm{unexplained}} = 1.7 \pm 0.7 \times 10^7$ molecules cm^{-3} s^{-1} (1σ) for low and high reactivity, respectively). Our hypothesis is that ozonolysis of VOCs could represent the missing OH source. Indeed, formation of OH from oxidation of unsaturated VOCs has been shown to be an important source of OH in winter, indoors and during night time (Paulson and Orlando, 1996; Geyer et al., 2003; Ren et al., 2003; Heard et al., 2004; Harrison et al., 2006; Johnson and Marston, 2008; Shallcross et al., 2014). As OH formation from ozonolysis proceeds through Criegee intermediates (Fig. 2), we can attempt to estimate a SCI concentration from the OH budget. First, we estimate from the unexplained OH production $P_{\mathrm{OH}}^{\mathrm{unexplained}}$ a so-called unexplained O_3 reactivity, $\sum(k_{\mathrm{VOC+O3}} \times [\mathrm{VOC_{unidentified}}])$, assuming a certain yield of OH from ozonolysis of unsaturated VOCs. Next, we estimate a yield of SCIs based on available literature data, and finally we combine both to estimate the SCI concentration required to close the OH budget. In contrast to the previous estimates, an average value is obtained for the SCIs, and not a time series, as we start from the average $P_{\mathrm{OH}}^{\mathrm{unexplained}}$, as reported in Hens et al. (2014).

Assuming that all unexplained OH production, $P_{\mathrm{OH}}^{\mathrm{unexplained}}$, comes from VOC ozonolysis with a certain OH yield Y_{OH}, we obtain

$$P_{\mathrm{OH}}^{\mathrm{unexplained}} = k_{\mathrm{voc+O_3}} \times [\mathrm{VOC_{unidentified}}] \times [\mathrm{O_3}] \times Y_{\mathrm{OH}}, \quad (5)$$

where $\mathrm{VOC_{unidentified}}$ includes the VOCs not considered in the OH budget performed by Hens et al. (2014), i.e. the VOCs causing the unknown OH reactivity discussed above. The average total OH yield from ozonolysis, Y_{OH}, is estimated at about 0.6 based on observed OH yields from the

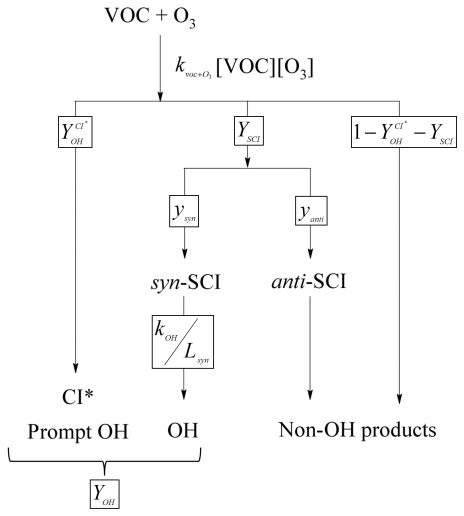

Figure 2. Schematic representation of the formation of OH from the ozonolysis of unsaturated VOCs.

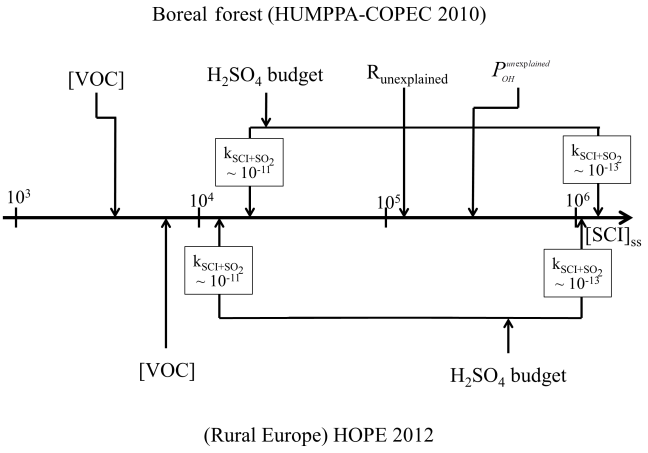

Figure 3. Schematic overview of the estimated steady-state concentration of SCIs ($[SCI]_{ss}$, molecules cm^{-3}) observed during the HUMPPA-COPEC 2010 and HOPE 2012 campaigns. For both campaigns the SCI estimate is based on the unsaturated VOC concentration measured, [VOC], and the H_2SO_4 budget using different $SCI + SO_2$ rate coefficients (k_{SCI+SO_2} in cm^3 molecule^{-1} s^{-1}). In addition, during the HUMPPA-COPEC campaign SCIs can be calculated from the unexplained OH reactivity, $R_{unexplained}$, and unexplained OH production, $P^{OH}_{unexplained}$. See main text for more details (Sect. 3).

literature (Atkinson et al., 2006). OH formation from ozonolysis occurs through two channels (Fig. 2): prompt formation by the decomposition of chemically activated CI* and delayed OH by formation of SCIs followed by their thermal decomposition; there are also product channels not yielding OH. The prompt yield of OH, $Y^{CI^*}_{OH}$ is estimated at ~ 0.4 from SCI scavenging experiments (Atkinson et al., 2004); the remaining yield Y^{SCI}_{OH} is then formed from SCIs, where $Y_{OH} = Y^{CI^*}_{OH} + Y^{SCI}_{OH}$ and hence $Y^{SCI}_{OH} \approx 0.2$.

We adopt a value for Y_{SCI} of 0.4, as argued in Sect. 3.2. The SCIs formed do not all decompose to OH, e.g. *anti*-CI tend to form esters instead. We label all SCIs able to yield OH as SCI_{syn}, without mandating a speciation but following the observation that *syn*-CI usually yield OH through the vinyl hydroperoxide channel. The total SCI yield is then divided into a fraction, Y_{syn}, forming SCI_{syn}, and the remainder, Y_{anti}, forming non-OH-generating SCIs. Little information is available on the $Y_{syn} : Y_{anti}$ ratio, with only a few theoretical calculations on smaller alkenes and a few monoterpenes (Rathman et al., 1999; Fenske et al., 2000b; Kroll et al., 2002; Nguyen et al., 2009a, b). For most of these compounds the ratio of *syn*- to *anti*-SCIs is between 0.2 and 1.0 (Rickard et al., 1999), where a larger fraction of *syn*- to *anti*-SCIs, or vice versa, will depend on the single alkene. As there is no information available for the VOCs included in this study, we estimate the ratio of Y_{syn} to Y_{anti} as 1 : 1. This number avoids overestimating the impact of SCIs in the OH production and, using the *syn* to *anti* range indicated above, would cause a variation in the final [SCI] estimate of maximum 20 % (see Eq. 7 and Fig. 3), well below the total uncertainty of the result.

The production of OH from SCI_{syn} formed from VOCs not included in the OH budget is then $k_{OH} \times [SCI_{syn}]$, where we estimate $k_{OH} \approx 20\,s^{-1}$ as measured by Novelli et al. (2014b) for *syn*-CH_3CHOO, and where the steady-state concentration of the SCI_{syn} , $[SCI_{syn}]$, is determined by the ratio of the formation processes and the sum L_{SCIsyn} of the loss processes already defined above:

$$[SCI_{syn}] = \frac{k_{voc+O_3} \times [VOC_{unidentified}] \times [O_3] \times Y_{SCI} \times Y_{syn}}{L_{SCI_{syn}}}. \quad (6)$$

Merging the above equations, expressing the measured OH production from unknown sources as the sum of direct OH production from CI* and indirect from SCI_{syn}, we obtain

$$P^{unexplained} = k_{voc+O_3} \times [VOC_{unidentified}] \times [O_3] \times \left(Y^{CI^*}_{OH} + Y_{SCI} \times Y_{syn} \times \frac{k_{OH}}{L_{SCI_{syn}}} \right). \quad (7)$$

The measured $P^{unexplained}_{OH}$ and $[O_3]$ and the estimates of the other parameters allow us to calculate the factor $k_{voc+O_3} \times [VOC_{unidentified}]$. Substituting this factor into Eq. (6) yields an estimate of the steady-state concentration of SCI_{syn}. With a value for $P^{unexplained}_{OH}$ of 1.0×10^6 molecules cm^{-3} s^{-1} as observed for low-reactivity episodes and at night during HUMPPA, a steady-state concentration of SCI_{syn} of $(2.0 \pm 2.0) \times 10^4$ molecules cm^{-3} is calculated. For high-reactivity episodes during HUMPPA-COPEC 2010, the missing $P^{unexplained}_{OH}$ of 2.0×10^7 molecules cm^{-3} s^{-1} results in a SCI concentration

of $(4.0 \pm 4.0) \times 10^5$ molecules cm^{-3}. To obtain the total SCI concentration, we then need to add the non-OH-producing SCIs. Here we assume that these are mostly *anti*-SCIs or H_2COO, both of which react rather quickly with H_2O or $(H_2O)_2$ (Taatjes et al., 2013; Chao et al., 2015; Lewis et al., 2015), and that their contribution can be neglected. We thus obtain that $[SCI] \approx [SCI_{syn}]$. To this we add the SCI concentration calculated from the measured unsaturated VOCs (Sect. 3.2), $(5.0 \pm 4.0) \times 10^3$ molecules cm^{-3}, to obtain the SCIs formed from all VOCs.

For HOPE 2012 it is difficult to accurately derive an OH budget due to the lack of information on the HONO concentration, which can represent an important primary source of OH. A detailed analysis of the OH production and loss during the campaign thus requires a detailed model study to derive HONO concentrations, which is outside the scope of this paper. Hence, an estimate on the SCIs from a possible missing OH production rate during the HOPE 2012 campaign is not included here.

Equation (7), for a given set of yields, unimolecular decomposition rates, and SCI losses, allows the estimate of the relative contribution of SCIs and CI* to the total production rate of OH from the ozonolysis of VOCs. With the yields considered in this study and for a unimolecular decomposition rate of SCIs into OH of 20 s^{-1}, the SCIs would contribute up to 12 % to the total formation of OH from ozonolysis of VOCs in both environments. This indicates that the SCIs do not have a large impact in the production of OH radicals and at the same time emphasises how important a realistic estimate of VOC concentration is for modelling the OH radical as already underlined by Hens et al. (2014).

3.5 Robustness of the [SCI] estimates

Figure 3 summarises the steady-state concentration of SCIs calculated on the basis of the H_2SO_4 budget, the measured unsaturated VOC concentration and OH reactivity (R), and the OH budget for the HUMPPA-COPEC 2010 and HOPE 2012 campaigns. By considering the lower and the highest values estimated from the measured VOCs and from the missing H_2SO_4 oxidant for both campaigns, respectively, the steady-state concentration of SCIs is calculated to be between 5.0×10^3 and 2.0×10^6 molecules cm^{-3} for the boreal forest environment during the HUMPPA-COPEC 2010 campaign and between 7.0×10^3 and 1.0×10^6 molecules cm^{-3} for rural Germany during the HOPE 2012 campaign (Table 2). The SCI concentrations calculated using these approaches represent a best-effort estimate made for the environments studied here based on the available data; due to the many uncertainties related to the chemistry of SCIs both in production and loss processes, these estimates span about 2 orders of magnitude.

The estimate of the SCI concentration from the sulfuric acid budgets relies on the rate of oxidation of SO_2 to H_2SO_4. As indicated in Sect. 3.1, two significantly different rate coefficients for the reaction of SCIs with SO_2 are currently available. One coefficient is high, $\sim 3.3 \pm 2.0 \times 10^{-11}$ cm^3 molecule^{-1} s^{-1}, while the other is several orders of magnitude lower, 5.0×10^{-13} cm^3 molecule^{-1} s^{-1}. Justifications of the differences in the values due to the diverse procedures, i.e. direct detection of $SCI + SO_2$ for the high rate coefficient and detection of H_2SO_4 for the lower one, are difficult, while recent measurements tend to agree with the highest value. This casts doubts on the highest obtained SCI concentrations of $\sim 10^6$ molecules cm^{-3}. In addition, the remaining three estimates strongly depend on the yield of SCIs, $k\mathrm{VOC} + \mathrm{O_3}$, and L_{SCIsyn}. Among these, the parameter with the highest uncertainty is the loss rate of *syn*-SCIs, L_{SCIsyn}, as it is based on relatively few studies, which report large differences between the observations. In this study, values of 40 s^{-1} and of 32 s^{-1}, based on previous model analysis (Novelli et al., 2014b), for the HUMPPA-COPEC 2010 and HOPE 2012 campaigns, respectively, were used. Recent work (Smith et al., 2016; Fang et al., 2016a; Long et al., 2016) suggests a faster unimolecular decomposition rate for the acetone oxide Criegee intermediate, exceeding 10^2 s^{-1} in ambient conditions. It is currently not clear whether this rate applies to more substituted SCIs as formed from monoterpenes, but the use of these higher decomposition rate in the model by Novelli et al. (2014b) would result in a total L_{SCIsyn} of ~ 110 s^{-1}. This loss rate would decrease the estimated SCI concentration by almost a factor of 3, closer to the lower estimates not exceeding 10^5 molecules cm^{-3}; this also casts doubt on the highest estimates given in Fig. 3. Therefore, an average estimated SCI concentration of about 5×10^4 molecules cm^{-3}, with an uncertainty of an order of magnitude, is considered more appropriate for both campaigns.

4 The source of the OH background signal

In this section we examine the background OH signal, OH_{bg} (Novelli et al., 2014b) measured during the two field campaigns discussed in the previous sections. In particular, we examine whether this signal is consistent with the SCI chemistry and concentrations indicated above.

4.1 Correlation of OH_{bg} with temperature

The time series of the background OH signal measured during the HUMPPA-COPEC 2010 and HOPE 2012 campaigns are shown together with temperature and $J(O^1D)$ values in Fig. 4. Increases and decreases in the OH_{bg} signal follow the temperature changes. During the HUMPPA-COPEC 2010 campaign the OH_{bg} shows a strong correlation with temperature (Fig. 5) with a correlation coefficient $R = 0.8$ for the exponential fit. The exponential dependency with temperature is in agreement with data shown by Di Carlo et al. (2004) for the unexplained OH reactivity and indicates

that the species responsible for the OH_{bg} strongly correlate with emission of biogenic VOCs (BVOCs) such as monoterpenes and sesquiterpenes, which have been shown to also exponentially depend on temperature (Guenther et al., 1993; Duhl et al., 2008; Hakola et al., 2003). This suggests that OH_{bg} is directly related to BVOC chemistry. The relationship between OH_{bg} and temperature during the HOPE 2012 campaign is less obvious. It is possible to observe a weakly exponential correlation between the two ($R = 0.51$, Fig. S10) but there is very large scatter in the data. It is worthwhile to underline the differences between the two environments. The forest in Finland is essentially pristine and BVOC-dominated, while in southern Germany a large fraction of non-biogenic VOCs was observed. The lack of a clear exponential correlation between OH_{bg} and temperature during the HOPE 2012 campaign could suggest different precursors or a different origin for the OH_{bg} within the two environments.

During both campaigns a negligible correlation, $R = 0.2$, was observed between background OH and $J(O^1D)$. This suggests that the OH_{bg} does not primarily originate from photolabile species.

4.2 Correlation of OH_{bg} with unexplained OH reactivity

As described in Sect. 3.3, during the HUMPPA-COPEC 2010 campaign high average OH reactivity was observed ($\sim 9\,s^{-1}$), of which between 60 and 90 % cannot be explained by the loss processes calculated from the measured species (Nölscher et al., 2012). A large unexplained fraction of the reactivity has often been observed, especially in forested environments (Di Carlo et al., 2004; Sinha et al., 2008; Edwards et al., 2013), indicating a large fraction of undetected BVOCs and/or secondary oxidation products. The OH_{bg} shows some correlation with the measured unexplained OH reactivity at 18 m, for the period on the ground ($R = 0.4$), and the measured unexplained OH reactivity at 24 m, for the period on the tower ($R = 0.4$) (Fig. 6). If we consider only night-time data, i.e. $J(O^1D) \leq 3.0 \times 10^{-6}\,s^{-1}$ (Hens et al., 2014), we obtain better agreement between the two datasets for both ground and tower periods. During the night a large fraction of observed OH production (Sect. 3.4) could not be explained, which can tentatively be attributed to formation of OH from ozonolysis of BVOCs, suggesting that the background OH could be related to such a process. Correlation between the OH_{bg} and the OH reactivity was also observed in a study by Mao et al. (2012) in a ponderosa pine plantation (California, Sierra Nevada) dominated by isoprene, where even higher OH reactivity was observed ($\sim 20\,s^{-1}$).

During the HOPE 2012 campaign such a correlation with the unexplained OH reactivity was not observed ($R = 0.1$). The OH reactivity was, on average, 3 times less than during the campaign in Finland and, as shown in Sect. 3.3, 50 % can be explained by reaction of OH with methane, formaldehyde, acetaldehyde, inorganic compounds (NO_x, SO_2, CO) and anthropogenic VOCs. On average only 17 % of the OH reactivity is caused by reaction of OH with BVOCs in this environment (Fig. S8), dropping to 10 % during the night. The unexplained OH reactivity is not influenced by distinguishing between day and night-time data, suggesting a small contribution of non-measured BVOCs. As this site is more strongly affected by anthropogenic emissions (Table S2) compared to the site in Finland, assuming that the OH_{bg} originates from

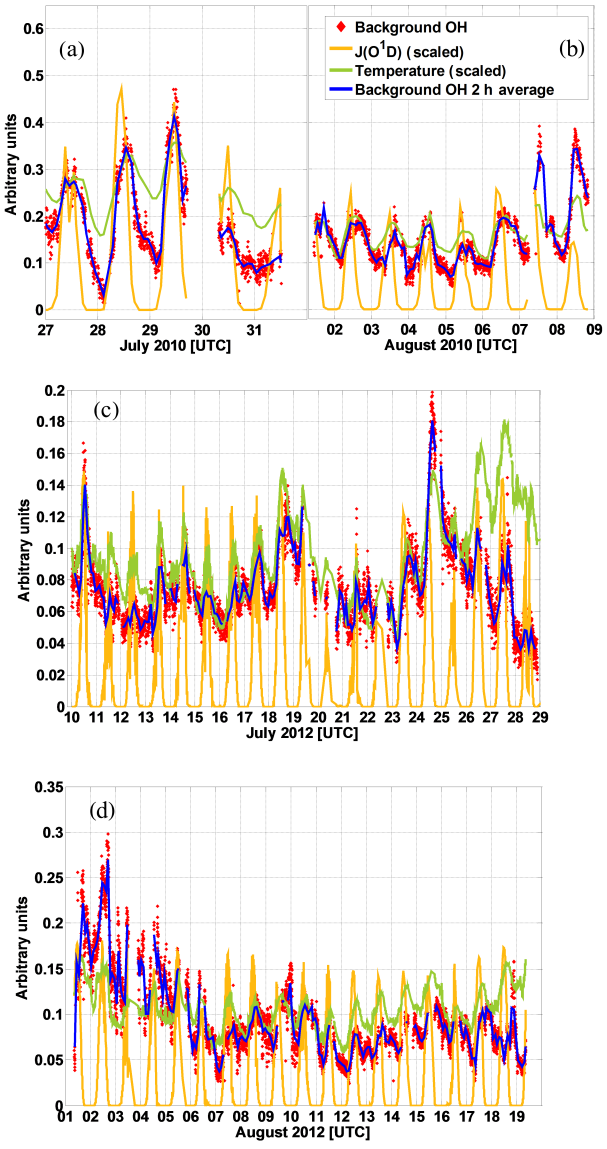

Figure 4. Background OH (red diamonds) measured during the HUMPPA-COPEC 2010 (**a**, ground; **b**, tower) and the HOPE 2012 (**c**, July; **d**, August) campaigns together with scaled $J(O^1D)$, multiplied by 4.0×10^4 and 4.0×10^3 for HUMPPA-COPEC 2010 and HOPE 2012, respectively (orange), and scaled temperature divided by 90 and 160 K for HUMPPA-COPEC 2010 and HOPE 2012, respectively (green).

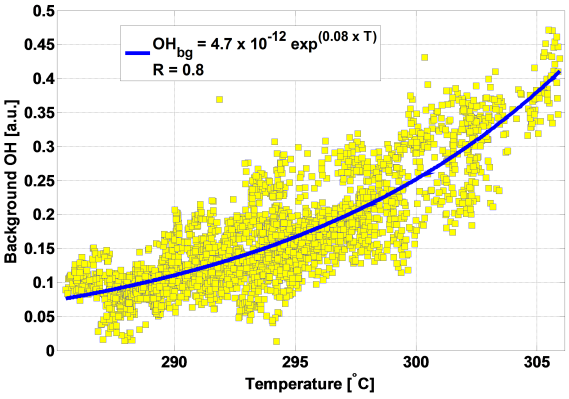

Figure 5. Background OH as a function of the temperature during the HUMPPA-COPEC 2010 campaign.

BVOC-driven chemistry, a lack of correlation between OH_{bg} and OH reactivity can be expected.

4.3 Correlation of OH_{bg} with ozonolysis chemistry

During the HUMMPA-COPEC 2010 campaign a high correlation with O_3, $R = 0.7$ (Fig. S11), indicates that background OH likely originates from ozonolysis processes. A comparison of background OH with the product of ozone concentration, measured unsaturated VOC concentration and their ozonolysis rate coefficient does not show the same relationship. No correlation ($R = 0.05$) is found by using the measured BVOC concentrations (Table S1). As most of the OH reactivity remains unexplained, with measured BVOCs comprising less than 10 % of the measured OH reactivity (Fig. S6, Table S2), the lack of correlation could suggest that the VOCs responsible for the formation of SCIs detected by the HORUS instrument are likely part of the large fraction of unmeasured species to which a correlation was reported in the previous section.

During HOPE 2012 a weak correlation was observed between background OH and ozone ($R = 0.5$, Fig. S12).

This campaign, from 10 July to 19 August 2012, encompasses a time period, from 1 to 3 August 2012, which was characterised by tree cutting in the vicinity of the measurement site. During this period a significantly larger fraction of unexplained OH reactivity, up to 40 % (Fig. S13), was observed. The relative contribution of measured BVOCs and inorganic compounds did not change, while the presence of unidentified BVOCs emitted from the trees as a result of the stress induced on the plants from the cutting activity caused the larger fraction of unexplained reactivity. Figure 7 shows the correlation between OH_{bg} and the product $k_{O_3}[VOC][O_3]$ of measured unsaturated VOC concentration (Table S1), $[O_3]$ and the relevant ozonolysis rate coefficients. The data points belonging to the tree-cutting period are depicted in red, which naturally correspond to a larger OH_{bg} concentration for similar concentrations of measured VOCs

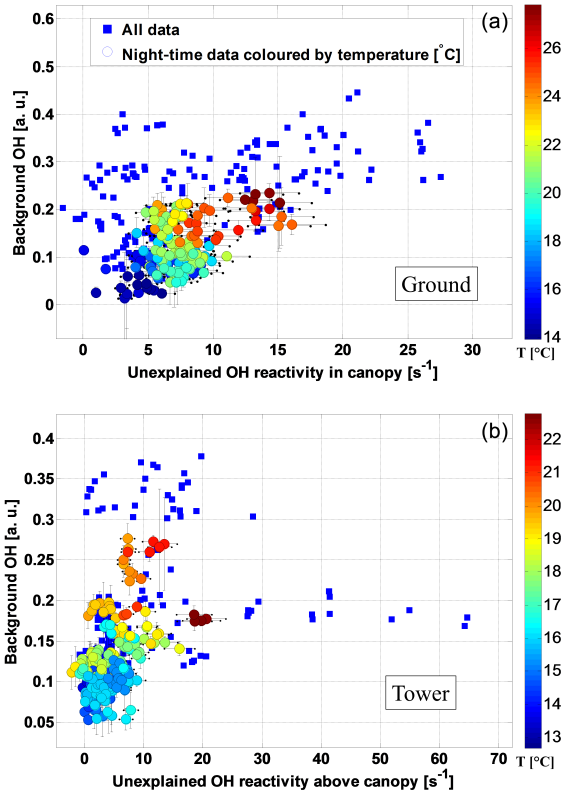

Figure 6. Background OH as a function of unexplained OH reactivity for ground and tower period measurements during the HUMPPA-COPEC 2010 campaign. Squares represent the daytime data; bullets represent night-time data and are coloured according to temperature (right legend).

during the rest of the campaign, as the additional contribution from the non-identified BVOCs is neglected. The overall correlation appears to be pretty poor in particular due to the few points scattering in the lower right corner. These points all belong to three consecutive days, from 26 to 28 July, which were characterised by high temperature and large concentrations of BVOCs (Table S3). As noticeable in Fig. 4, during those 3 days the OH_{bg} strongly deviates from the temperature trends and reaches lower values. At present, the reason for such a low concentration of OH_{bg}, during a period which should favour its formation if it originates from SCIs, is unclear. The instrument was left unattended at the site and the drop in the quality of the signals required its shutdown on the evening of 28 July. However, as no evidence was found to suggest an error in the data, the points have not been omitted. Excluding that period yields a correlation factor of $R = 0.65$. The correlation line intercept could arise for a number of reasons. Unmeasured components of the OH reactivity (i.e. unspeciated VOCs) are not accounted for in the calculation, and doing so would shift the data to higher [VOC], decreasing the positive intercept. This is also consistent with a higher intercept for the tree-cutting period, where a larger unexplained

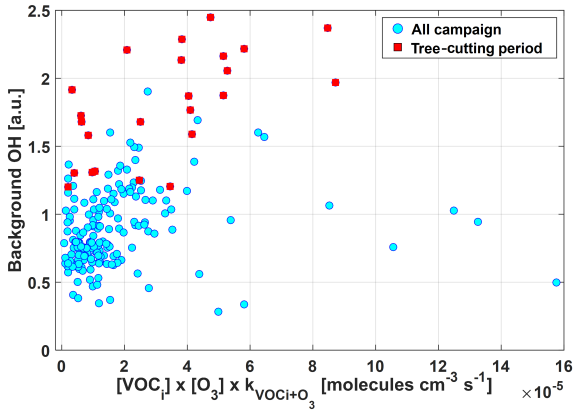

Figure 7. Background OH as a function of the sum of the product of the measured unsaturated VOC–ozone turn-over (Table S1), during the HOPE 2012 campaign. The blue points refer to the entire field campaign excluding tree cutting, which occurred between 1 and 3 August 2012, described by the red squares.

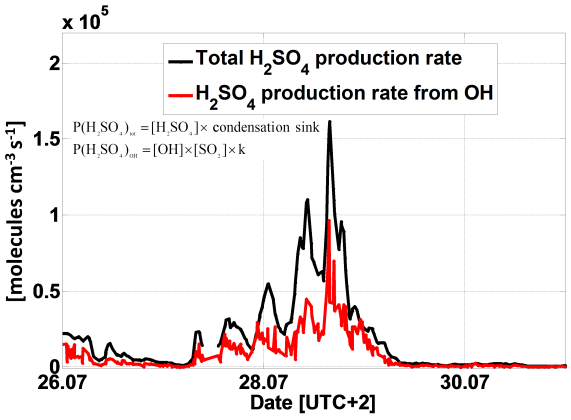

Figure 8. Comparison of the total H_2SO_4 production rate (black line), calculated from the measured H_2SO_4, and the production rate of H_2SO_4 (red line) involving only the oxidation process of SO_2 by OH for the ground measurements during the HUMPPA-COPEC 2010 campaign.

OH reactivity was observed. It is also conceivable that the intercept is in part due to an additional, non-ozonolysis source of background OH. One candidate for the night-time periods could be NO_3 as found in the work by Fuchs et al. (2016). Unfortunately, there was no measurement of the NO_3 radical during the HOPE 2012 campaign, but based on previous studies at the site (Handisides et al., 2003), a concentration up to 14 pptv of NO_3 could be present and could have a detectable impact.

Apart from the possible partial origin of OH_{bg} from NO_3 or other interferences, there are also indications that the background OH could originate from ozonolysis of unsaturated biogenic compounds. The correlation analysis requires that all VOCs are accounted for, and omitting large contributions from unspeciated VOCs, as evidenced , for example, by OH reactivity measurements, can be expected to reduce the correlation as observed in the case of HUMPPA-COPEC 2010. The reason for the lack of correlation during the period from 26 to 28 July 2012 during HOPE-2012 characterised by large BVOC emissions remains unclear.

4.4 Correlation of OH_{bg} with $P(H_2SO_4)_{unex}$

During both campaigns, measurements of H_2SO_4, SO_2, OH, and CS (condensation sink) were performed, allowing the calculation of the sulfuric acid budget in the gas phase. As shown by Mauldin III et al. (2012), during the HUMPPA-COPEC 2010 campaign the well-known SO_2 oxidation process by OH (Wayne, 2000) (Eq. 1) was not sufficient to explain the measured concentration of H_2SO_4. As shown in Sect. 3.1, half of the production rate of H_2SO_4, $\sim 1 \times 10^4$ molecules cm^{-3} s^{-1}, cannot be explained by reaction with OH radicals (Fig. 8). The missing oxidant is assumed to be SCIs, as discussed in Sect. 3.1, because of their fast reaction rate with SO_2. As our hypothesis about the origin of the OH_{bg} supports this assumption, we compared the $[H_2SO_4]_{unex}$ observed during the HUMPPA-COPEC 2010 campaign with the OH_{bg} multiplied by SO_2 for the ground-based period when the instruments (HORUS and CIMS) measured side by side (Fig. 9). The two datasets indicate a correlation coefficient of $R = 0.6$, suggesting that whichever species is responsible for the oxidation of SO_2 is related to the formation of OH within the HORUS instrument.

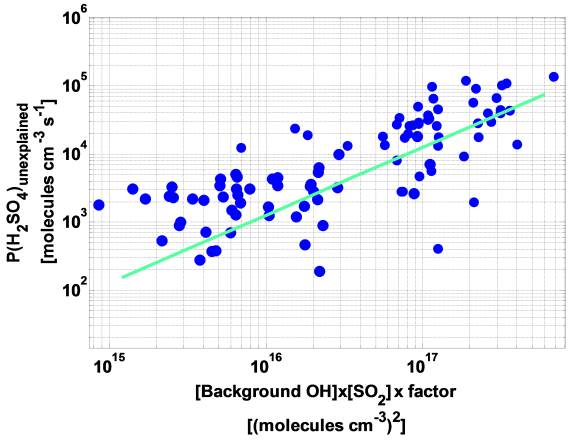

Figure 9. The production rate of H_2SO_4 unaccounted for by the oxidation of SO_2 by OH as a function of the OH_{bg} multiplied by SO_2 concentration during the ground measurements of the HUMPPA-COPEC 2010 campaign. OH_{bg} is expressed in molecules cm^{-3} equivalents of OH.

Note that for the HOPE 2012 campaign the same budget calculation shows only a small fraction (10 %) of unexplained H_2SO_4 production rate (Fig. 1).

If we assuming SCIs to be the unknown SO_2 oxidant, the results observed in both campaigns are in agreement with the modelling study by Boy et al. (2013), who analysed mea-

surements at the same sites described in this study. Similar to our result, they found a larger contribution of SCIs in the formation of H_2SO_4 for the boreal forest compared to rural Germany. As the OH concentration differs by, on average, less than 50 % between the two environments, a similar concentration of SCIs in HOPE to that calculated for HUMPPA-COPEC 2010 would contribute up to 30 % in the formation of H_2SO_4. However, the H_2SO_4 budget during this campaign can approximately be closed by only considering the measured OH concentrations, suggesting that the concentration of SCIs in this environment is smaller than that during the HUMPPA-COPEC 2010 campaign. This is consistent with the calculation in Sect. 3 based on the smaller reactivity and hence smaller VOC concentration in this environment.

4.5 Scavenging experiments

A series of scavenging tests of the OH_{bg} was performed during the HOPE 2012 campaign to help identify the interfering species. SO_2 was chosen as a scavenger for the species causing the OH_{bg}, as it has been shown in several laboratory studies to react quickly with SCIs ($k \sim 3.3 \times 10^{-11}$ cm^3 molecule^{-1} s^{-1}) mostly independently of their structure (Taatjes et al., 2014). The injection of SO_2 was performed through the IPI system (Novelli et al., 2014a) together with an OH scavenger. First the OH scavenger propane was injected within the IPI to remove the atmospheric OH; subsequently, SO_2 was injected in addition to the OH scavenger (Fig. 10). A set of experiments were performed at the end of the campaign, resulting in the depletion of the OH_{bg} signal as shown in Fig. 10. The concentration of SO_2 is small enough not to scavenge SCIs inside the low-pressure section of the instrument, nor is it additionally removing atmospheric OH within the IPI system as the lifetime of OH by reaction with SO_2 is 200 times that of propane. With the addition of SO_2 (1×10^{13} molecules cm^{-3} in the sampled air) it is possible to suppress the OH_{bg} signal from the instrument to within the zero noise, indicating that the OH_{bg} signal originates from an SCI-like species that reacts with SO_2 and decomposes unimolecularly to OH. Similar results were obtained in later field campaigns; this will be discussed in the pertaining upcoming publications. Note that it is not possible to link the signal strength directly to an OH or precursor concentration, as analysed in the following section.

4.6 SCIs as a source of background OH

During the HUMPPA-COPEC 2010 campaign the background OH showed a strong exponential relationship with temperature ($R = 0.8$) and it correlates with unexplained OH reactivity ($R = 0.5$), which suggests correlation with BVOCs, ozone ($R = 0.7$), and also the $P(H_2SO_4)_{unex}$ ($R = 0.6$). During the HOPE 2012 campaign a weak exponential correlation with temperature was recognised

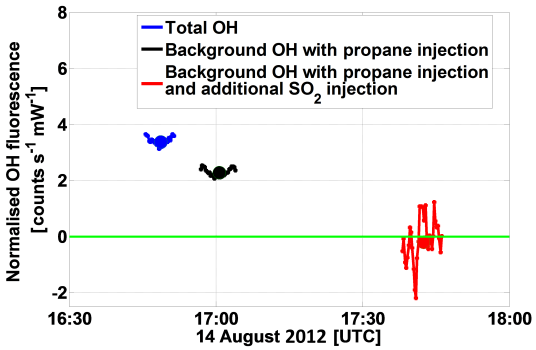

Figure 10. SO_2 injection test within IPI during the HOPE 2012 campaign. The blue data points represent the total OH measured when no injection is performed. The black data points represent the background OH measured while injecting propane (2.5×10^{15} molecules cm^{-3}) scavenging > 90 % of ambient OH. The red signal is the background OH observed when SO_2 (1.0×10^{13} molecules cm^{-3}) is injected in addition to propane.

($R = 0.5$), but no correlation was observed with OH reactivity. The OH_{bg} correlated with the product of ozone and unsaturated VOCs for most of the campaign ($R = 0.6$), although not for a period of 3 days at the end of July with partly higher BVOC–O_3 turnover. In addition, during HOPE 2012 the OH_{bg} signal was scavenged by the addition of SO_2.

All evidence presented indicates that substantial parts of the OH_{bg} originate from a species formed during the ozonolysis of unsaturated VOCs that decomposes into OH, is removable by SO_2 and, if present in a significant concentration, increases the H_2SO_4 production. We are currently not aware of any chemical species, other than SCIs, known to oxidise SO_2 at a fast enough rate and also decompose into OH. In addition, HORUS was shown to be sensitive to the OH formed after unimolecular decomposition of SCIs in the low-pressure region of the instrument (residence time 2 ms) in controlled laboratory studies (Novelli et al., 2014b). During the HUMPPA-COPEC 2010 campaign, the correlation with OH reactivity improved when considering only data during night time, the period during which a higher fraction of the production rate of OH could not be accounted for (Hens et al., 2014). Indeed, during the night recycling via $HO_2 + NO$ is low due to the negligible NO concentration; therefore, a different path of formation of OH is expected. One likely path could be the formation of OH from excited and stabilised CIs formed from ozonolysis of unsaturated compounds.

The considerations above are all consistent with the hypothesis that OH_{bg} largely originates from unimolecular decomposition of SCIs in the field as well as in the laboratory.

Attempts to analyse the absolute concentration of SCIs based on our OH_{bg}, however, indicate that this hypothesis is not without difficulties. A particular problem is that to date no method is available to produce and quantify a known concentration of a specific SCI conformer, which

precludes the absolute calibration of SCI-generated OH. A priori, it seems unlikely that the IPI-LIF-FAGE instrument calibration factor for ambient OH, i.e. sampled from outside the instrument through the nozzle, is identical to the sensitivity for OH generated inside. The transmission factor through our nozzle pinhole is currently not known for OH radicals; the calibration factor used for ambient OH accounts for this transmission as well as, for example, OH losses on the walls, alignment of the white cell, transmission optics, and response of the MCP. These last three factors should affect the OH generated from any interfering species similarly, while wall losses and transmission through the pinhole are different and possibly also differ between SCI conformers. Additionally, different SCIs vary in their unimolecular decomposition rates and hence affect calibration by a different time-specific OH yield. For example, theoretical studies (Vereecken and Francisco, 2012) and laboratory experiments (Smith et al., 2016) indicate that acetone oxide will decompose faster than *syn*-acetaldehyde oxide, causing the formation of a different amount of OH, which in turn will also be affected by different loss rates in the low-pressure segment of the instrument. Thus, it is not possible to convert the internal OH to an absolute SCI concentration since the mixture of SCIs is not known. At best one could obtain an "average" sensitivity factor, if one knew the OH_{bg} formed from a series of reference SCI conformers, and if the ambient SCI speciation is known and not too strongly dependent on reaction conditions. To further illustrate the need of a SCI-specific calibration, we try to simply calculate the external [SCI] from the internal OH_{bg} signal strength, calibrated based on the combined experimental and modelling study by Novelli et al. (2014b). For a SCI mixture that behaves identically to syn-CH_3CHOO, the OH_{bg} from the HUMPPA-COPEC 2010 campaign would then indicate an external [SCI] $\geq 2 \times 10^7$ molecules cm^{-3}, well above the estimates presented in Sect. 3. Moreover, the observed OH_{bg} signal interpreted in this way would imply an ambient OH production exceeding 4×10^8 molecules cm^{-3} s^{-1}, clearly in disagreement with known chemistry, and also inconsistent with our estimates (Table 2). If we assume a faster decomposition rate for the SCIs of 200 s^{-1}, a higher fraction of the SCI decomposes in the low-pressure region, i.e. 80 % compared to 25 % for $k_{uni} = 20\,s^{-1}$. This leads to a higher OH signal per SCI, and from this a [SCI] of 4.0×10^6 molecules cm^{-3}, though the implied ambient OH production would remain significantly too high. Thus, the conversion of the OH signal to an absolute concentration of ambient SCIs is not unambiguous without full SCI speciation and knowledge of their chemical kinetics. Note, furthermore, that these [SCI] estimates would represent a lower limit as we only observe SCIs that decompose to OH, whereas, for example, *anti*-SCIs convert to acids/esters.

In an effort to work towards SCI-specific calibration, we probed the transmission of OH and *syn*-CH_3CHOO through the nozzles and the low-pressure region in the instrument, with explorative laboratory tests using a traditional nozzle and a molecular beam skimmer nozzle, where the latter has much thinner sidewalls and a significantly narrower gas expansion, strongly reducing wall contact. The laboratory test showed that the OH radical has a 23 % higher transmission through the molecular beam nozzle compared to the traditional nozzle. The *syn*-acetaldehyde oxide did not show any statistical difference in the transmission between the two nozzles. This indicates that (a) SCIs and OH have a different transmission efficiency and most likely different wall losses, underlining that the OH calibration factor is not applicable to SCIs for ambient measurements, and (b) that the calibration factor for OH obtained for ambient OH alone does not allow the quantification of the absolute OH concentration in the low-pressure section of the FAGE instrument. This is the fundamental reason why the earlier simple estimate of [SCI] and OH production leads to strong overestimations.

In addition to the above effects, one should also consider that OH production from SCIs in the low-pressure section might be catalysed to proceed at rates beyond their ambient counterpart, biasing our interpretation of their ambient fate. The catalysis might involve wall-induced isomerisation of the higher-energy *anti*-SCIs to the more stable, OH-producing *syn*-SCIs, which would artificially increase the *syn* : *anti* ratio. Another possibility is the evaporation of clusters stabilising the SCIs, as it is known that SCIs efficiently form complexes with many compounds, including water, acids, alcohols, hydroperoxides, HO_x radicals, etc. (Vereecken and Francisco, 2012). Redissociation of secondary ozonides (SOZs) seems less important, except perhaps the SOZs formed with CO_2 (Aplincourt and Ruiz-López, 2000), which has no alternative accessible unimolecular channels. At present, insufficient (if any) information is available to assess the impact of such catalysis.

Taking into account the factors considered above, and assuming that the estimates for the SCI concentration in both environments are correct, it appears unlikely that SCIs are responsible for such a large OH_{bg} signal as observed by the HORUS instrument. If SCIs were to be solely responsible for the OH_{bg} signal, the HORUS instrument would need to be far more sensitive to the detection of SCIs than to the detection of OH radicals by, for example, pinhole losses that are 100 times smaller for SCIs than for OH radicals. The evident discrepancy between the qualitative evidence in support of the SCI hypothesis and the current quantitative difficulty in reconciling the OH_{bg} signal with the estimated ambient concentration of SCIs does not allow an unequivocal identification of the origin of the OH_{bg} within our system. It cannot be excluded that multiple species are contributing to the OH_{bg} signal. NO_3 chemistry during night time has been identified as a possible source of OH_{bg} in the LIF-FAGE instrument of the FZ-Jülich (Fuchs et al., 2016). However, in the case of the large observed night-time OH_{bg} concentrations during HUMPPA-COPEC 2010, the measured night-time NO_3

concentrations were below 1 ppt and therefore too small to explain the observed OH_{bg}.

5 Conclusions

We estimated a steady-state concentration of SCIs for the HUMPPA-COPEC 2010 and the HOPE 2012 campaigns based on a large dataset. Starting from four different approaches, i.e. based on unaccounted (i.e. non-OH) H_2SO_4 oxidant, measured VOC concentrations, unexplained OH reactivity, or unexplained production rates of OH, we estimated the concentration of SCIs to be between $\sim 10^3$ and $\sim 10^6$ molecules cm^{-3}. The highest values in this range are linked to an assumed low rate coefficient for $SCI + SO_2$ of 5.0×10^{-13} cm^3 $molecule^{-1}$ s^{-1} (see Sect. 3.1), which is at odds with a larger body of more direct measurements on this rate coefficient. Hence, higher SCI values appear to be relatively less likely. We thus obtain an average SCI concentration of about 5.0×10^4 molecules cm^{-3}, with an order of magnitude uncertainty, for both campaigns. At such concentrations, SCIs are expected to have a significant impact on H_2SO_4 chemistry during the HUMPPA-COPEC 2010 campaign, while during the HOPE 2012 campaign their impact is much smaller and possibly negligible. Additionally, it was shown that, based on the yields and unimolecular decomposition rate applied in this study, SCIs do not have a large impact on the OH production compared to the direct OH generation from ozonolysis of unsaturated VOCs. During both campaigns, the IPI-LIF-FAGE instrument detected an OH background signal that originates from decomposition of one or more species inside the low-pressure region of the instrument. The source compound of the OH_{bg} was shown to be unreactive towards propane but to be removed by SO_2, and a relationship was found with the unaccounted H_2SO_4 production rate. It correlates with temperature in the same way as the emission of terpenes and, in most but not all measurements periods, with the product of unsaturated VOCs and ozone as well as with the OH reactivity. While it is not possible at the moment to unequivocally state that OH_{bg} originates from stabilised Criegee intermediates, the observations are consistent with known SCI chemistry. The contribution of SCIs to the observed OH_{bg} cannot be quantified until a calibration scheme for SCIs in the IPI-FAGE system has been developed.

The predicted SCI concentrations derived in this study are low, likely not exceeding 10^5 molecules cm^{-3}; therefore, the presence of SCIs is unlikely to have a large impact on atmospheric chemistry; the main exception appears to be H_2SO_4 production in selected environments.

Data availability. The data of this paper are available upon request. Please contact the corresponding author, Hartwig Harder (h.harder@mpic.de).

The Supplement related to this article is available online at https://doi.org/10.5194/acp-17-7807-2017-supplement.

Competing interests. The authors declare that they have no conflict of interest.

Acknowledgements. Luc Vereecken was supported by the Max Planck Graduate Centre (MPGC) with the Johannes Gutenberg-Universität Mainz.

Work during HUMPPA-COPEC was supported by the Hyytiälä site engineers and staff. Support of the European Community Research Infrastructure Action under the FP6 "Structuring the European Research Area" programme, EUSAAR contract no. RII3-CT-2006-026140, is gratefully acknowledged. The HUMPPA-COPEC 2010 campaign measurements and analyses were supported by the ERC grant ATMNUCLE (project no. 227463), the Academy of Finland Centre of Excellence programme (project no. 1118615), the Academy of Finland Centre of Excellence in Atmospheric Science – From Molecular and Biological processes to The Global Climate (ATM, 272041), the European integrated project on Aerosol Cloud Climate and Air Quality Interactions (EUCAARI, project no. 036833-2), the EUSAAR TNA (project no. 400586), and the IMECC TA (project No. 4006261).

The work during HOPE 2012 was supported by the scientists and staff of DWD Hohenpeißenberg, whom we would like to thank for providing the "platform" and opportunity to perform such a campaign. In particular, we thank Anja Werner, Jennifer Englert, and Katja Michl for the VOC measurements, Stephan Gilge for the trace gases measurements, and Georg Stange for running the CIMS.

We also would like to thank Markus Rudolf for much technical support and guidance, Eric Regelin and Umar Javed for the numerous scientific discussions, Petri Keronen for providing meteorological and trace gas concentration data from Hyytiälä during the HUMPPA-COPEC 2010 and Thorsten Berndt for providing the data to re-evaluate the rate coefficient between SCIs and SO_2.

The article processing charges for this open-access publication were covered by the Max Planck Society.

Edited by: Kyung-Eun Min
Reviewed by: two anonymous referees

References

Aalto, P., Hämeri, K., Becker, E. D. O., Weber, R., Salm, J., Mäkelä, J. M., Hoell, C., O'Dowd, C. D., Karlsson, H., Hansson, H.-C., Väkevä, M., Koponen, I. K., Buzorius, G., and Kulmala, M.: Physical characterization of aerosol particles during nucleation events, Tellus B, 53, 344–358, https://doi.org/10.1034/j.1600-0889.2001.530403.x, 2001.

Ahrens, J., Carlsson, P. T., Hertl, N., Olzmann, M., Pfeifle, M., Wolf, J. L., and Zeuch, T.: Infrared detection of Criegee intermediates formed during the ozonolysis of beta-pinene and their reactivity towards sulfur dioxide, Angew. Chem. Int. Edit., 53, 715–719, https://doi.org/10.1002/anie.201307327, 2014.

Amédro, D.: Atmospheric measurements of OH and HO_2 radicals using FAGE : Development and deployment on the field, Université Lille1 – Sciences et Technologies, Tokyo Metropolitan University, 2012.

Anglada, J. M., Bofill, J. M., Olivella, S., and Solé, A.: Unimolecular Isomerizations and Oxygen Atom Loss in Formaldehyde and Acetaldehyde Carbonyl Oxides. A Theoretical Investigation, J. Am. Chem. Soc., 118, 4636–4647, https://doi.org/10.1021/ja953858a, 1996.

Anglada, J. M., Gonzalez, J., and Torrent-Sucarrat, M.: Effects of the substituents on the reactivity of carbonyl oxides. A theoretical study on the reaction of substituted carbonyl oxides with water, Phys. Chem. Chem. Phys., 13, 13034–13045, 2011.

Anglada, J. M. and Sole, A.: Impact of water dimer on the atmospheric reactivity of carbonyl oxides, Phys. Chem. Chem. Phys., 18, 17698–17712 , https://doi.org/10.1039/C6CP02531E, 2016.

Aplincourt, P. and Ruiz-López, M. F.: Theoretical Investigation of Reaction Mechanisms for Carboxylic Acid Formation in the Atmosphere, J. Am. Chem. Soc., 122, 8990–8997, https://doi.org/10.1021/ja000731z, 2000.

Atkinson, R., Baulch, D. L., Cox, R. A., Crowley, J. N., Hampson, R. F., Hynes, R. G., Jenkin, M. E., Rossi, M. J., and Troe, J.: Evaluated kinetic and photochemical data for atmospheric chemistry: Volume I – gas phase reactions of O_x, HO_x, NO_x and SO_x species, Atmos. Chem. Phys., 4, 1461–1738, https://doi.org/10.5194/acp-4-1461-2004, 2004.

Atkinson, R., Baulch, D. L., Cox, R. A., Crowley, J. N., Hampson, R. F., Hynes, R. G., Jenkin, M. E., Rossi, M. J., Troe, J., and IUPAC Subcommittee: Evaluated kinetic and photochemical data for atmospheric chemistry: Volume II – gas phase reactions of organic species, Atmos. Chem. Phys., 6, 3625–4055, https://doi.org/10.5194/acp-6-3625-2006, 2006.

Berndt, T., Jokinen, T., Mauldin, R. L., Petaja, T., Herrmann, H., Junninen, H., Paasonen, P., Worsnop, D. R., and Sipila, M.: Gas-Phase Ozonolysis of Selected Olefins: The Yield of Stabilized Criegee Intermediate and the Reactivity toward SO_2, J. Phys. Chem. Lett., 3, 2892–2896, https://doi.org/10.1021/jz301158u, 2012.

Berndt, T., Jokinen, T., Sipilä, M., Mauldin Iii, R. L., Herrmann, H., Stratmann, F., Junninen, H., and Kulmala, M.: H_2SO_4 formation from the gas-phase reaction of stabilized Criegee Intermediates with SO_2: Influence of water vapour content and temperature, Atmos. Environ., 89, 603–612, https://doi.org/10.1016/j.atmosenv.2014.02.062, 2014a.

Berndt, T., Voigtlander, J., Stratmann, F., Junninen, H., Mauldin Iii, R. L., Sipila, M., Kulmala, M., and Herrmann, H.: Competing atmospheric reactions of CH_2OO with SO_2 and water vapour, Phys. Chem. Chem. Phys., 16, 19130–19136, https://doi.org/10.1039/c4cp02345e, 2014b.

Berresheim, H., Elste, T., Plass-Dülmer, C., Eisele, F. L., and Tanner, D. J.: Chemical ionization mass spectrometer for long-term measurements of atmospheric OH and H_2SO_4, Int. J. Mass Spectrom., 202, 91–109, https://doi.org/10.1016/S1387-3806(00)00233-5, 2000.

Birmili, W., Berresheim, H., Plass-Dülmer, C., Elste, T., Gilge, S., Wiedensohler, A., and Uhrner, U.: The Hohenpeissenberg aerosol formation experiment (HAFEX): a long-term study including size-resolved aerosol, H_2SO_4, OH, and monoterpenes measurements, Atmos. Chem. Phys., 3, 361–376, https://doi.org/10.5194/acp-3-361-2003, 2003.

Boy, M., Mogensen, D., Smolander, S., Zhou, L., Nieminen, T., Paasonen, P., Plass-Dülmer, C., Sipilä, M., Petäjä, T., Mauldin, L., Berresheim, H., and Kulmala, M.: Oxidation of SO_2 by stabilized Criegee intermediate (sCI) radicals as a crucial source for atmospheric sulfuric acid concentrations, Atmos. Chem. Phys., 13, 3865–3879, https://doi.org/10.5194/acp-13-3865-2013, 2013.

Buras, Z. J., Elsamra, R. M., Jalan, A., Middaugh, J. E., and Green, W. H.: Direct kinetic measurements of reactions between the simplest Criegee intermediate CH_2OO and alkenes, J. Phys. Chem. A, 118, 1997–2006, https://doi.org/10.1021/jp4118985, 2014.

Chao, W., Hsieh, J.-T., Chang, C.-H., and Lin, J. J.-M.: Direct kinetic measurement of the reaction of the simplest Criegee intermediate with water vapor, Science, 347, 751–754, https://doi.org/10.1126/science.1261549, 2015.

Chen, L., Wang, W., Wang, W., Liu, Y., Liu, F., Liu, N., and Wang, B.: Water-catalyzed decomposition of the simplest Criegee intermediate CH_2OO, Theor. Chem. Acc., 135, 1–13, https://doi.org/10.1007/s00214-016-1894-9, 2016.

Chhantyal-Pun, R., Davey, A., Shallcross, D. E., Percival, C. J., and Orr-Ewing, A. J.: A kinetic study of the CH_2OO Criegee intermediate self-reaction, reaction with SO_2 and unimolecular reaction using cavity ring-down spectroscopy, Phys. Chem. Chem. Phys., 17, 3617–3626, https://doi.org/10.1039/c4cp04198d, 2015.

Criegee, R.: Mechanism of Ozonolysis, Angew. Chem. Int. Edit., 14, 745–752, https://doi.org/10.1002/anie.197507451, 1975.

Di Carlo, P., Brune, W. H., Martinez, M., Harder, H., Lesher, R., Ren, X. R., Thornberry, T., Carroll, M. A., Young, V., Shepson, P. B., Riemer, D., Apel, E., and Campbell, C.: Missing OH reactivity in a forest: Evidence for unknown reactive biogenic VOCs, Science, 304, 722–725, https://doi.org/10.1126/science.1094392, 2004.

Donahue, N. M., Drozd, G. T., Epstein, S. A., Presto, A. A., and Kroll, J. H.: Adventures in ozoneland: down the rabbit-hole, Phys. Chem. Chem. Phys., 13, 10848–10857, https://doi.org/10.1039/c0cp02564j, 2011.

Drozd, G. T. and Donahue, N. M.: Pressure Dependence of Stabilized Criegee Intermediate Formation from a Sequence of Alkenes, J. Phys. Chem. A, 115, 4381–4387, https://doi.org/10.1021/jp2001089, 2011.

Drozd, G. T., Kroll, J., and Donahue, N. M.: 2,3-Dimethyl-2-butene (TME) Ozonolysis: Pressure Dependence of Stabilized Criegee Intermediates and Evidence of Stabilized Vinyl Hydroperoxides, J. Phys. Chem. A, 115, 161–166, https://doi.org/10.1021/jp108773d, 2011.

Duhl, T. R., Helmig, D., and Guenther, A.: Sesquiterpene emissions from vegetation: a review, Biogeosciences, 5, 761–777, https://doi.org/10.5194/bg-5-761-2008, 2008.

Edwards, P. M., Evans, M. J., Furneaux, K. L., Hopkins, J., Ingham, T., Jones, C., Lee, J. D., Lewis, A. C., Moller, S. J., Stone, D., Whalley, L. K., and Heard, D. E.: OH reactivity in a South East Asian tropical rainforest during the Oxidant and Particle Photochemical Processes (OP3) project, Atmos. Chem. Phys., 13, 9497–9514, https://doi.org/10.5194/acp-13-9497-2013, 2013.

Fang, Y., Liu, F., Barber, V. P., Klippenstein, S. J., McCoy, A. B., and Lester, M. I.: Communication: Real time

observation of unimolecular decay of Criegee intermediates to OH radical products, J. Chem. Phys., 144, 061102, https://doi.org/10.1063/1.4941768, 2016a.

Fang, Y., Liu, F., Klippenstein, S. J., and Lester, M. I.: Direct observation of unimolecular decay of CH_3CH_2CHOO Criegee intermediates to OH radical products, J. Chem. Phys., 145, 044312, https://doi.org/10.1063/1.4958992, 2016b.

Fenske, J. D., Hasson, A. S., Ho, A. W., and Paulson, S. E.: Measurement of Absolute Unimolecular and Bimolecular Rate Constants for CH_3CHOO Generated by the trans-2-Butene Reaction with Ozone in the Gas Phase, J. Phys. Chem. A, 104, 9921–9932, https://doi.org/10.1021/jp0016636, 2000a.

Fenske, J. D., Kuwata, K. T., Houk, K. N., and Paulson, S. E.: OH Radical Yields from the Ozone Reaction with Cycloalkenes, J. Phys. Chem. A, 104, 7246–7254, https://doi.org/10.1021/jp993611q, 2000b.

Foreman, E. S., Kapnas, K. M., and Murray, C.: Reactions between Criegee Intermediates and the Inorganic Acids HCl and HNO_3: Kinetics and Atmospheric Implications, Angew. Chem. Int. Edit., 55, 10419–10422, https://doi.org/10.1002/anie.201604662, 2016.

Fuchs, H., Tan, Z., Hofzumahaus, A., Broch, S., Dorn, H.-P., Holland, F., Künstler, C., Gomm, S., Rohrer, F., Schrade, S., Tillmann, R., and Wahner, A.: Investigation of potential interferences in the detection of atmospheric RO_x radicals by laser-induced fluorescence under dark conditions, Atmos. Meas. Tech., 9, 1431–1447, https://doi.org/10.5194/amt-9-1431-2016, 2016.

Geyer, A., Bächmann, K., Hofzumahaus, A., Holland, F., Konrad, S., Klüpfel, T., Pätz, H.-W., Perner, D., Mihelcic, D., Schäfer, H.-J., Volz-Thomas, A., and Platt, U.: Nighttime formation of peroxy and hydroxyl radicals during the BERLIOZ campaign: Observations and modeling studies, J. Geophys. Res.-Atmos., 108, 8249, https://doi.org/10.1029/2001jd000656, 2003.

Gilge, S., Plass-Duelmer, C., Fricke, W., Kaiser, A., Ries, L., Buchmann, B., and Steinbacher, M.: Ozone, carbon monoxide and nitrogen oxides time series at four alpine GAW mountain stations in central Europe, Atmos. Chem. Phys., 10, 12295–12316, https://doi.org/10.5194/acp-10-12295-2010, 2010.

Griffith, S. M., Hansen, R. F., Dusanter, S., Stevens, P. S., Alaghmand, M., Bertman, S. B., Carroll, M. A., Erickson, M., Galloway, M., Grossberg, N., Hottle, J., Hou, J., Jobson, B. T., Kammrath, A., Keutsch, F. N., Lefer, B. L., Mielke, L. H., O'Brien, A., Shepson, P. B., Thurlow, M., Wallace, W., Zhang, N., and Zhou, X. L.: OH and HO_2 radical chemistry during PROPHET 2008 and CABINEX 2009 – Part 1: Measurements and model comparison, Atmos. Chem. Phys., 13, 5403–5423, https://doi.org/10.5194/acp-13-5403-2013, 2013.

Griffith, S. M., Hansen, R. F., Dusanter, S., Michoud, V., Gilman, J. B., Kuster, W. C., Veres, P. R., Graus, M., de Gouw, J. A., Roberts, J., Young, C., Washenfelder, R., Brown, S. S., Thalman, R., Waxman, E., Volkamer, R., Tsai, C., Stutz, J., Flynn, J. H., Grossberg, N., Lefer, B., Alvarez, S. L., Rappenglueck, B., Mielke, L. H., Osthoff, H. D., and Stevens, P. S.: Measurements of hydroxyl and hydroperoxy radicals during CalNex-LA: Model comparisons and radical budgets, J. Geophys. Res.-Atmos., 121, 4211–4232, https://doi.org/10.1002/2015JD024358, 2016.

Guenther, A. B., Zimmerman, P. R., Harley, P. C., Monson, R. K., and Fall, R.: Isoprene and monoterpene emission rate variability: Model evaluations and sensitivity analyses, J. Geophys. Res.-Atmos., 98, 12609–12617, https://doi.org/10.1029/93jd00527, 1993.

Hakola, H., Tarvainen, V., Laurila, T., Hiltunen, V., Hellén, H., and Keronen, P.: Seasonal variation of VOC concentrations above a boreal coniferous forest, Atmos. Environ., 37, 1623–1634, https://doi.org/10.1016/S1352-2310(03)00014-1, 2003.

Handisides, G. M., Plass-Dülmer, C., Gilge, S., Bingemer, H., and Berresheim, H.: Hohenpeissenberg Photochemical Experiment (HOPE 2000): Measurements and photostationary state calculations of OH and peroxy radicals, Atmos. Chem. Phys., 3, 1565–1588, https://doi.org/10.5194/acp-3-1565-2003, 2003.

Harrison, R. M., Yin, J., Tilling, R. M., Cai, X., Seakins, P. W., Hopkins, J. R., Lansley, D. L., Lewis, A. C., Hunter, M. C., Heard, D. E., Carpenter, L. J., Creasey, D. J., Lee, J. D., Pilling, M. J., Carslaw, N., Emmerson, K. M., Redington, A., Derwent, R. G., Ryall, D., Mills, G., and Penkett, S. A.: Measurement and modelling of air pollution and atmospheric chemistry in the U.K. West Midlands conurbation: Overview of the PUMA Consortium project, Sci. Total Environ., 360, 5–25, https://doi.org/10.1016/j.scitotenv.2005.08.053, 2006.

Hasson, A. S., Ho, A. W., Kuwata, K. T., and Paulson, S. E.: Production of stabilized Criegee intermediates and peroxides in the gas phase ozonolysis of alkenes: 2. Asymmetric and biogenic alkenes, J. Geophys. Res.-Atmos., 106, 34143–34153, https://doi.org/10.1029/2001jd000598, 2001.

Heard, D. E., Carpenter, L. J., Creasey, D. J., Hopkins, J. R., Lee, J. D., Lewis, A. C., Pilling, M. J., Seakins, P. W., Carslaw, N., and Emmerson, K. M.: High levels of the hydroxyl radical in the winter urban troposphere, Geophys. Res. Lett., 31, L18112, https://doi.org/10.1029/2004gl020544, 2004.

Hens, K., Novelli, A., Martinez, M., Auld, J., Axinte, R., Bohn, B., Fischer, H., Keronen, P., Kubistin, D., Nölscher, A. C., Oswald, R., Paasonen, P., Petäjä, T., Regelin, E., Sander, R., Sinha, V., Sipilä, M., Taraborrelli, D., Tatum Ernest, C., Williams, J., Lelieveld, J., and Harder, H.: Observation and modelling of HO_x radicals in a boreal forest, Atmos. Chem. Phys., 14, 8723–8747, https://doi.org/10.5194/acp-14-8723-2014, 2014.

Hoerger, C. C., Claude, A., Plass-Duelmer, C., Reimann, S., Eckart, E., Steinbrecher, R., Aalto, J., Arduini, J., Bonnaire, N., Cape, J. N., Colomb, A., Connolly, R., Diskova, J., Dumitrean, P., Ehlers, C., Gros, V., Hakola, H., Hill, M., Hopkins, J. R., Jäger, J., Junek, R., Kajos, M. K., Klemp, D., Leuchner, M., Lewis, A. C., Locoge, N., Maione, M., Martin, D., Michl, K., Nemitz, E., O'Doherty, S., Pérez Ballesta, P., Ruuskanen, T. M., Sauvage, S., Schmidbauer, N., Spain, T. G., Straube, E., Vana, M., Vollmer, M. K., Wegener, R., and Wenger, A.: ACTRIS non-methane hydrocarbon intercomparison experiment in Europe to support WMO GAW and EMEP observation networks, Atmos. Meas. Tech., 8, 2715–2736, https://doi.org/10.5194/amt-8-2715-2015, 2015.

Horie, O., Neeb, P., and Moortgat, G. K.: The reactions of the Criegee intermediate CH_3CHOO in the gas-phase ozonolysis of 2-butene isomers, Int. J. Chem. Kinet., 29, 461–468, https://doi.org/10.1002/(sici)1097-4601(1997)29:6<461::aid-kin8>3.0.co;2-s, 1997.

Horie, O., Schäfer, C., and Moortgat, G. K.: High reactivity of hexafluoroacetone toward criegee intermediates in the gas-phase ozonolysis of simple alkenes, Int. J. Chem. Kinet., 31, 261–269, https://doi.org/10.1002/(sici)1097-4601(1999)31:4<261::aid-kin3>3.0.co;2-z, 1999.

Huang, H.-L., Chao, W., and Lin, J. J.-M.: Kinetics of a Criegee intermediate that would survive high humidity and may oxidize atmospheric SO_2, P. Natl. Acad. Sci. USA, 112, 10857–10862, https://doi.org/10.1073/pnas.1513149112, 2015.

Jiang, L., Xu, Y.-S., and Ding, A.-Z.: Reaction of Stabilized Criegee Intermediates from Ozonolysis of Limonene with Sulfur Dioxide: Ab Initio and DFT Study, J. Phys. Chem. A, 114, 12452–12461, https://doi.org/10.1021/jp107783z, 2010.

Johnson, D. and Marston, G.: The gas-phase ozonolysis of unsaturated volatile organic compounds in the troposphere, Chem. Soc. Rev., 37, 699–716, 2008.

Junninen, H., Lauri, A., Keronen, P., Aalto, P., Hiltunen, V., Hari, P., and Kulmala, M.: Smart-SMEAR: on-line data exploration and visualization tool for SMEAR stations, Boreal Env. Res., 14, 447–457, 2009.

Kidwell, N. M., Li, H., Wang, X., Bowman, J. M., and Lester, M. I.: Unimolecular dissociation dynamics of vibrationally activated CH_3CHOO Criegee intermediates to OH radical products, Nat. Chem., advance online publication, https://doi.org/10.1038/nchem.2488, available at: http://www.nature.com/nchem/journal/vaop/ncurrent/abs/nchem.2488.html#supplementary-information, last access: 11 April 2016.

Kroll, J. H., Sahay, S. R., Anderson, J. G., Demerjian, K. L., and Donahue, N. M.: Mechanism of HO_x Formation in the Gas-Phase Ozone-Alkene Reaction. 2. Prompt versus Thermal Dissociation of Carbonyl Oxides to Form OH, J. Phys. Chem. A, 105, 4446–4457, https://doi.org/10.1021/jp004136v, 2001.

Kroll, J. H., Donahue, N. M., Cee, V. J., Demerjian, K. L., and Anderson, J. G.: Gas-Phase Ozonolysis of Alkenes: Formation of OH from Anti Carbonyl Oxides, J. Am. Chem. Soc., 124, 8518–8519, https://doi.org/10.1021/ja0266060, 2002.

Kulmala, M., Maso, M. D., MäKelä, J. M., Pirjola, L., VäKevä, M., Aalto, P., Miikkulainen, P., HäMeri, K., and O'Dowd, C. D.: On the formation, growth and composition of nucleation mode particles, Tellus B, 53, 479–490, https://doi.org/10.1034/j.1600-0889.2001.530411.x, 2001.

Kurteìn, T., Lane, J. R., Jørgensen, S., and Kjaergaard, H. G.: A Computational Study of the Oxidation of SO_2 to SO_3 by Gas-Phase Organic Oxidants, J. Phys. Chem. A, 115, 8669–8681, https://doi.org/10.1021/jp203907d, 2011.

Kuwata, K. T., Hermes, M. R., Carlson, M. J., and Zogg, C. K.: Computational studies of the isomerization and hydration reactions of acetaldehyde oxide and methyl vinyl carbonyl oxide, J. Phys. Chem. A, 114, 9192–9204, https://doi.org/10.1021/jp105358v, 2010.

Lee, Y.-P.: Perspective: Spectroscopy and kinetics of small gaseous Criegee intermediates, J. Chem. Phys., 143, 020901, https://doi.org/10.1063/1.4923165, 2015.

Lewis, T. R., Blitz, M., Heard, D. E., and Seakins, P.: Direct evidence for a substantive reaction between the C1 Criegee radical, CH_2OO, and the water vapour dimer, Phys. Chem. Chem. Phys., 17, 4859–4863, https://doi.org/10.1039/c4cp04750h, 2015.

Lin, L.-C., Chang, H.-T., Chang, C.-H., Chao, W., Smith, M. C., Chang, C.-H., Min Lin Jr., J., and Takahashi, K.: Competition between H_2O and $(H_2O)_2$ reactions with CH_2OO/CH_3CHOO, Phys. Chem. Chem. Phys., 18, 4557–4568, https://doi.org/10.1039/C5CP06446E, 2016.

Liu, F., Beames, J. M., Green, A. M., and Lester, M. I.: UV spectroscopic characterization of dimethyl- and ethyl-substituted carbonyl oxides, J. Phys. Chem. A, 118, 2298–2306, https://doi.org/10.1021/jp412726z, 2014a.

Liu, Y., Bayes, K. D., and Sander, S. P.: Measuring rate constants for reactions of the simplest Criegee intermediate (CH_2OO) by monitoring the OH radical, J. Phys. Chem. A, 118, 741–747, https://doi.org/10.1021/jp407058b, 2014b.

Long, B., Bao, J. L., and Truhlar, D. G.: Atmospheric Chemistry of Criegee Intermediates. Unimolecular Reactions and Reactions with Water, J. Am. Chem. Soc., 138, 14409–14422, https://doi.org/10.1021/jacs.6b08655, 2016.

Mao, J., Ren, X., Zhang, L., Van Duin, D. M., Cohen, R. C., Park, J.-H., Goldstein, A. H., Paulot, F., Beaver, M. R., Crounse, J. D., Wennberg, P. O., DiGangi, J. P., Henry, S. B., Keutsch, F. N., Park, C., Schade, G. W., Wolfe, G. M., Thornton, J. A., and Brune, W. H.: Insights into hydroxyl measurements and atmospheric oxidation in a California forest, Atmos. Chem. Phys., 12, 8009–8020, https://doi.org/10.5194/acp-12-8009-2012, 2012.

Martinez, M., Harder, H., Kubistin, D., Rudolf, M., Bozem, H., Eerdekens, G., Fischer, H., Klüpfel, T., Gurk, C., Königstedt, R., Parchatka, U., Schiller, C. L., Stickler, A., Williams, J., and Lelieveld, J.: Hydroxyl radicals in the tropical troposphere over the Suriname rainforest: airborne measurements, Atmos. Chem. Phys., 10, 3759–3773, https://doi.org/10.5194/acp-10-3759-2010, 2010.

Mauldin III, R. L., Berndt, T., Sipila, M., Paasonen, P., Petaja, T., Kim, S., Kurten, T., Stratmann, F., Kerminen, V. M., and Kulmala, M.: A new atmospherically relevant oxidant of sulphur dioxide, Nature, 488, 193–196, 2012.

Newland, M. J., Rickard, A. R., Alam, M. S., Vereecken, L., Munoz, A., Rodenas, M., and Bloss, W. J.: Kinetics of stabilised Criegee intermediates derived from alkene ozonolysis: reactions with SO_2, H_2O and decomposition under boundary layer conditions, Phys. Chem. Chem. Phys., 17, 4076–4088, https://doi.org/10.1039/c4cp04186k, 2015a.

Newland, M. J., Rickard, A. R., Vereecken, L., Muñoz, A., Ródenas, M., and Bloss, W. J.: Atmospheric isoprene ozonolysis: impacts of stabilised Criegee intermediate reactions with SO_2, H_2O and dimethyl sulfide, Atmos. Chem. Phys., 15, 9521–9536, https://doi.org/10.5194/acp-15-9521-2015, 2015b.

Nguyen, T. L., Peeters, J., and Vereecken, L.: Theoretical study of the gas-phase ozonolysis of β-pinene ($C_{10}H_{16}$), Phys. Chem. Chem. Phys., 11, 5643–5656, https://doi.org/10.1039/b822984h, 2009a.

Nguyen, T. L., Winterhalter, R., Moortgat, G., Kanawati, B., Peeters, J., and Vereecken, L.: The gas-phase ozonolysis of β-caryophyllene (C15H24). Part II: A theoretical study, Phys. Chem. Chem. Phys., 11, 4173–4183, 2009b.

Nölscher, A. C., Williams, J., Sinha, V., Custer, T., Song, W., Johnson, A. M., Axinte, R., Bozem, H., Fischer, H., Pouvesle, N., Phillips, G., Crowley, J. N., Rantala, P., Rinne, J., Kulmala, M., Gonzales, D., Valverde-Canossa, J., Vogel, A., Hoffmann, T., Ouwersloot, H. G., Vilà-Guerau de Arellano, J., and Lelieveld, J.: Summertime total OH reactivity measurements from boreal forest during HUMPPA-COPEC 2010, Atmos. Chem. Phys., 12, 8257–8270, https://doi.org/10.5194/acp-12-8257-2012, 2012.

Novelli, A., Hens, K., Tatum Ernest, C., Kubistin, D., Regelin, E., Elste, T., Plass-Dülmer, C., Martinez, M., Lelieveld, J.,

and Harder, H.: Characterisation of an inlet pre-injector laser-induced fluorescence instrument for the measurement of atmospheric hydroxyl radicals, Atmos. Meas. Tech., 7, 3413–3430, https://doi.org/10.5194/amt-7-3413-2014, 2014a.

Novelli, A., Vereecken, L., Lelieveld, J., and Harder, H.: Direct observation of OH formation from stabilised Criegee intermediates, Phys. Chem. Chem. Phys., 16, 19941–19951, https://doi.org/10.1039/c4cp02719a, 2014b.

Ouyang, B., McLeod, M. W., Jones, R. L., and Bloss, W. J.: NO_3 radical production from the reaction between the Criegee intermediate CH_2OO and NO_2, Phys. Chem. Chem. Phys., 15, 17070–17075, https://doi.org/10.1039/c3cp53024h, 2013.

Paulson, S. E. and Orlando, J. J.: The reactions of ozone with alkenes: An important source of HO_x in the boundary layer, Geophys. Res. Lett., 23, 3727–3730, https://doi.org/10.1029/96gl03477, 1996.

Paulson, S. E., Chung, M. Y., and Hasson, A. S.: OH Radical Formation from the Gas-Phase Reaction of Ozone with Terminal Alkenes and the Relationship between Structure and Mechanism, J. Phys. Chem. A, 103, 8125–8138, https://doi.org/10.1021/jp991995e, 1999.

Peeters, J., Boullart, W., Pultau, V., Vandenberk, S., and Vereecken, L.: Structure-Activity Relationship for the Addition of OH to (Poly)alkenes: Site-Specific and Total Rate Constants, J. Phys. Chem. A, 111, 1618–1631, https://doi.org/10.1021/jp066973o, 2007.

Percival, C. J., Welz, O., Eskola, A. J., Savee, J. D., Osborn, D. L., Topping, D. O., Lowe, D., Utembe, S. R., Bacak, A., McFiggans, G., Cooke, M. C., Xiao, P., Archibald, A. T., Jenkin, M. E., Derwent, R. G., Riipinen, I., Mok, D. W., Lee, E. P., Dyke, J. M., Taatjes, C. A., and Shallcross, D. E.: Regional and global impacts of Criegee intermediates on atmospheric sulphuric acid concentrations and first steps of aerosol formation, Faraday Discuss., 165, 45–73, https://doi.org/10.1039/c3fd00048f, 2013.

Petäjä, T., Mauldin, III, R. L., Kosciuch, E., McGrath, J., Nieminen, T., Paasonen, P., Boy, M., Adamov, A., Kotiaho, T., and Kulmala, M.: Sulfuric acid and OH concentrations in a boreal forest site, Atmos. Chem. Phys., 9, 7435–7448, https://doi.org/10.5194/acp-9-7435-2009, 2009.

Pierce, J. R., Evans, M. J., Scott, C. E., D'Andrea, S. D., Farmer, D. K., Swietlicki, E., and Spracklen, D. V.: Weak global sensitivity of cloud condensation nuclei and the aerosol indirect effect to Criegee + SO_2 chemistry, Atmos. Chem. Phys., 13, 3163–3176, https://doi.org/10.5194/acp-13-3163-2013, 2013.

Plass-Dülmer, C., Michl, K., Ruf, R., and Berresheim, H.: C_2–C_8 Hydrocarbon measurement and quality control procedures at the Global Atmosphere Watch Observatory Hohenpeissenberg, J. Chromatogr. A, 953, 175–197, https://doi.org/10.1016/S0021-9673(02)00128-0, 2002.

Rathman, W. C. D., Claxton, T. A., Rickard, A. R., and Marston, G.: A theoretical investigation of OH formation in the gas-phase ozonolysis of E-but-2-ene and Z-but-2-ene, Phys. Chem. Chem. Phys., 1, 3981–3985, https://doi.org/10.1039/a903186c, 1999.

Ren, X., Harder, H., Martinez, M., Lesher, R. L., Oliger, A., Simpas, J. B., Brune, W. H., Schwab, J. J., Demerjian, K. L., He, Y., Zhou, X., and Gao, H.: OH and HO_2 Chemistry in the urban atmosphere of New York City, Atmos. Environ., 37, 3639–3651, https://doi.org/10.1016/S1352-2310(03)00459-X, 2003.

Rickard, A. R., Johnson, D., McGill, C. D., and Marston, G.: OH Yields in the Gas-Phase Reactions of Ozone with Alkenes, J. Phys. Chem. A, 103, 7656–7664, https://doi.org/10.1021/jp9916992, 1999.

Ryzhkov, A. B. and Ariya, P. A.: A theoretical study of the reactions of carbonyl oxide with water in atmosphere: the role of water dimer, Chem. Phys. Lett., 367, 423–429, https://doi.org/10.1016/S0009-2614(02)01685-8, 2003.

Ryzhkov, A. B. and Ariya, P. A.: A theoretical study of the reactions of parent and substituted Criegee intermediates with water and the water dimer, Phys. Chem. Chem. Phys., 6, 5042–5050, https://doi.org/10.1039/b408414d, 2004.

Sarwar, G., Fahey, K., Kwok, R., Gilliam, R. C., Roselle, S. J., Mathur, R., Xue, J., Yu, J., and Carter, W. P. L.: Potential impacts of two SO_2 oxidation pathways on regional sulfate concentrations: Aqueous-phase oxidation by NO_2 and gas-phase oxidation by Stabilized Criegee Intermediates, Atmos. Environ., 68, 186–197, https://doi.org/10.1016/j.atmosenv.2012.11.036, 2013.

Sarwar, G., Simon, H., Fahey, K., Mathur, R., Goliff, W. S., and Stockwell, W. R.: Impact of sulfur dioxide oxidation by Stabilized Criegee Intermediate on sulfate, Atmos. Environ., 85, 204–214, https://doi.org/10.1016/j.atmosenv.2013.12.013, 2014.

Shallcross, D. E., Taatjes, C. A., and Percival, C. J.: Criegee intermediates in the indoor environment: new insights, Indoor Air, 24, 495–502, https://doi.org/10.1111/ina.12102, 2014.

Sheps, L., Scully, A. M., and Au, K.: UV absorption probing of the conformer-dependent reactivity of a Criegee intermediate CH_3CHOO, Phys. Chem. Chem. Phys., 16, 26701–26706, https://doi.org/10.1039/c4cp04408h, 2014.

Shillings, A. J. L., Ball, S. M., Barber, M. J., Tennyson, J., and Jones, R. L.: An upper limit for water dimer absorption in the 750 nm spectral region and a revised water line list, Atmos. Chem. Phys., 11, 4273–4287, https://doi.org/10.5194/acp-11-4273-2011, 2011.

Sinha, V., Williams, J., Crowley, J. N., and Lelieveld, J.: The Comparative Reactivity Method – a new tool to measure total OH Reactivity in ambient air, Atmos. Chem. Phys., 8, 2213–2227, https://doi.org/10.5194/acp-8-2213-2008, 2008.

Sipilä, M., Jokinen, T., Berndt, T., Richters, S., Makkonen, R., Donahue, N. M., Mauldin III, R. L., Kurtén, T., Paasonen, P., Sarnela, N., Ehn, M., Junninen, H., Rissanen, M. P., Thornton, J., Stratmann, F., Herrmann, H., Worsnop, D. R., Kulmala, M., Kerminen, V.-M., and Petäjä, T.: Reactivity of stabilized Criegee intermediates (sCIs) from isoprene and monoterpene ozonolysis toward SO2 and organic acids, Atmos. Chem. Phys., 14, 12143–12153, https://doi.org/10.5194/acp-14-12143-2014, 2014.

Smith, M. C., Chang, C.-H., Chao, W., Lin, L.-C., Takahashi, K., Boering, K. A., and Lin, J. J.-M.: Strong Negative Temperature Dependence of the Simplest Criegee Intermediate CH_2OO Reaction with Water Dimer, The Journal of Physical Chemistry Letters, 6, 2708–2713, https://doi.org/10.1021/acs.jpclett.5b01109, 2015.

Smith, M. C., Chao, W., Takahashi, K., Boering, K. A., and Lin, J. J.-M.: Unimolecular Decomposition Rate of the Criegee Intermediate $(CH_3)_2COO$ Measured Directly with UV Absorption Spectroscopy, J. Phys. Chem. A, 120, 4789–4798, https://doi.org/10.1021/acs.jpca.5b12124, 2016.

Stone, D., Blitz, M., Daubney, L., Howes, N. U., and Seakins, P.: Kinetics of CH_2OO reactions with SO_2, NO_2, NO, H_2O and

CH_3CHO as a function of pressure, Phys. Chem. Chem. Phys., 16, 1139–1149, https://doi.org/10.1039/c3cp54391a, 2014.

Taatjes, C. A., Welz, O., Eskola, A. J., Savee, J. D., Scheer, A. M., Shallcross, D. E., Rotavera, B., Lee, E. P., Dyke, J. M., Mok, D. K., Osborn, D. L., and Percival, C. J.: Direct measurements of conformer-dependent reactivity of the Criegee intermediate CH_3CHOO, Science, 340, 177–180, https://doi.org/10.1126/science.1234689, 2013.

Taatjes, C. A., Shallcross, D. E., and Percival, C. J.: Research frontiers in the chemistry of Criegee intermediates and tropospheric ozonolysis, Phys. Chem. Chem. Phys., 16, 1704–1718, https://doi.org/10.1039/c3cp52842a, 2014.

Tan, Z., Fuchs, H., Lu, K., Hofzumahaus, A., Bohn, B., Broch, S., Dong, H., Gomm, S., Häseler, R., He, L., Holland, F., Li, X., Liu, Y., Lu, S., Rohrer, F., Shao, M., Wang, B., Wang, M., Wu, Y., Zeng, L., Zhang, Y., Wahner, A., and Zhang, Y.: Radical chemistry at a rural site (Wangdu) in the North China Plain: observation and model calculations of OH, HO_2 and RO_2 radicals, Atmos. Chem. Phys., 17, 663–690, https://doi.org/10.5194/acp-17-663-2017, 2017.

Tobias, H. J. and Ziemann, P. J.: Kinetics of the Gas-Phase Reactions of Alcohols, Aldehydes, Carboxylic Acids, and Water with the C13 Stabilized Criegee Intermediate Formed from Ozonolysis of 1-Tetradecene, J. Phys. Chem. A, 105, 6129–6135, https://doi.org/10.1021/jp004631r, 2001.

Vereecken, L. and Francisco, J. S.: Theoretical studies of atmospheric reaction mechanisms in the troposphere, Chem. Soc. Rev., 41, 6259–6293, https://doi.org/10.1039/c2cs35070j, 2012.

Vereecken, L., Harder, H., and Novelli, A.: The reaction of Criegee intermediates with NO, RO_2, and SO_2, and their fate in the atmosphere, Phys. Chem. Chem. Phys., 14, 14682–14695, https://doi.org/10.1039/c2cp42300f, 2012.

Vereecken, L., Harder, H., and Novelli, A.: The reactions of Criegee intermediates with alkenes, ozone, and carbonyl oxides, Phys. Chem. Chem. Phys., 16, 4039–4049, https://doi.org/10.1039/c3cp54514h, 2014.

Vereecken, L., Glowacki, D. R., and Pilling, M. J.: Theoretical Chemical Kinetics in Tropospheric Chemistry: Methodologies and Applications, Chem. Rev., 115, 4063–4114, https://doi.org/10.1021/cr500488p, 2015.

Wayne, R. P.: Chemistry of Atmosphere, Oxford University Press, Oxford, 2000.

Welz, O., Savee, J. D., Osborn, D. L., Vasu, S. S., Percival, C. J., Shallcross, D. E., and Taatjes, C. A.: Direct Kinetic Measurements of Criegee Intermediate (CH_2OO) Formed by Reaction of CH_2I with O_2, Science, 335, 204–207, https://doi.org/10.1126/science.1213229, 2012.

White, J. U.: Long optical paths of large aperture, J. Opt. Soc. Am., 32, 285–288, https://doi.org/10.1364/josa.32.000285, 1942.

Williams, J., Crowley, J., Fischer, H., Harder, H., Martinez, M., Petäjä, T., Rinne, J., Bäck, J., Boy, M., Dal Maso, M., Hakala, J., Kajos, M., Keronen, P., Rantala, P., Aalto, J., Aaltonen, H., Paatero, J., Vesala, T., Hakola, H., Levula, J., Pohja, T., Herrmann, F., Auld, J., Mesarchaki, E., Song, W., Yassaa, N., Nölscher, A., Johnson, A. M., Custer, T., Sinha, V., Thieser, J., Pouvesle, N., Taraborrelli, D., Tang, M. J., Bozem, H., Hosaynali-Beygi, Z., Axinte, R., Oswald, R., Novelli, A., Kubistin, D., Hens, K., Javed, U., Trawny, K., Breitenberger, C., Hidalgo, P. J., Ebben, C. J., Geiger, F. M., Corrigan, A. L., Russell, L. M., Ouwersloot, H. G., Vilà-Guerau de Arellano, J., Ganzeveld, L., Vogel, A., Beck, M., Bayerle, A., Kampf, C. J., Bertelmann, M., Köllner, F., Hoffmann, T., Valverde, J., González, D., Riekkola, M.-L., Kulmala, M., and Lelieveld, J.: The summertime Boreal forest field measurement intensive (HUMPPA-COPEC-2010): an overview of meteorological and chemical influences, Atmos. Chem. Phys., 11, 10599–10618, https://doi.org/10.5194/acp-11-10599-2011, 2011.

Woodward-Massey, R., Cryer, D. R., Whalley, L. K., Ingham, T., Seakins, P. W., Heard, D. E., and Stimpson, L. M.: Implementation of a chemical background method (OH-CHEM) for measurements of OH using the Leeds FAGE instrument: Characterisation and observations from a coastal location. , Abstract A41A-0002 presented at 2015 Fall Meeting, AGU, San Francisco, Calif., 14–18 December 2015.

Yassaa, N., Song, W., Lelieveld, J., Vanhatalo, A., Bäck, J., and Williams, J.: Diel cycles of isoprenoids in the emissions of Norway spruce, four Scots pine chemotypes, and in Boreal forest ambient air during HUMPPA-COPEC-2010, Atmos. Chem. Phys., 12, 7215–7229, https://doi.org/10.5194/acp-12-7215-2012, 2012.

York, D., Evensen, N. M., Martínez, M. L., and De Basabe Delgado, J.: Unified equations for the slope, intercept, and standard errors of the best straight line, Am. J. Phys., 72, 367–375, https://doi.org/10.1119/1.1632486, 2004.

Zhang, D. and Zhang, R.: Mechanism of OH Formation from Ozonolysis of Isoprene: A Quantum-Chemical Study, J. Am. Chem. Soc., 124, 2692–2703, https://doi.org/10.1021/ja011518l, 2002.

Zhu, C., Kumar, M., Zhong, J., Li, L., Francisco, J. S., and Zeng, X. C.: New Mechanistic Pathways for Criegee–Water Chemistry at the Air/Water Interface, J. Am. Chem. Soc., 138, 11164–11169, https://doi.org/10.1021/jacs.6b04338, 2016.